Calhoun
Institutional Archive of the Naval Postgraduate School

Calhoun: The NPS Institutional Archive

DSpace Repository

Theses and Dissertations | 1. Thesis and Dissertation Collection, all items

1956

The longitudinal frequency response of a Navion airplane from steady state dynamic testing utilizing simplified instruments

Ekas, Claude P.; Prichard, Reuben P.; Townsend, Marland W.

Princeton University

http://hdl.handle.net/10945/14379

Downloaded from NPS Archive: Calhoun

DUDLEY KNOX LIBRARY

Calhoun is the Naval Postgraduate School's public access digital repository for research materials and institutional publications created by the NPS community. Calhoun is named for Professor of Mathematics Guy K. Calhoun, NPS's first appointed -- and published -- scholarly author.

Dudley Knox Library / Naval Postgraduate School
411 Dyer Road / 1 University Circle
Monterey, California USA 93943

http://www.nps.edu/library

THE LONGITUDINAL FREQUENCY RESPONSE OF A NAVION AIRPLANE FROM A STEADY STATE DYNAMIC TESTING UTILIZING SIMPLIFIED INSTRUMENTATION

Claude P. Ekas, Jr.
Reuben P. Prichard Jr.
and
Marland W. Townsend, Jr.

Library
U. S. Naval Postgraduate School
Monterey, California

1-54

AIW	AIRPLANE
FRE	FREQUENCY RESPONSE
TES	TEST

THE LONGITUDINAL FREQUENCY RESPONSE OF A NAVION AIRPLANE FROM STEADY STATE DYNAMIC TESTING UTILIZING SIMPLIFIED INSTRUMENTATION

Lieutenant Claude P. Ekas, Jr., USN
Lieutenant Reuben P. Prichard, Jr., USN
Lieutenant Marland W. Townsend, Jr., USN

Aeronautical Engineering Report No. 348
June 1, 1956

Thesis
E [illegible] 6

ACKNOWLEDGEMENTS

The authors wish to express their gratitude for the opportunities and facilities provided by Princeton University in the undertaking of this thesis project in the field of airplane dynamics. The authors also wish to express their appreciation to Professor Courtland D. Perkins, under whose guidance and supervision the project was carried out.

The authors are also indebted to Mr. Enoch Durbin for his aid in the initial instrumentation, to Mr. C. P. Ekas for manufacturing several items of equipment for oscillating the elevator, and to Mr. Robert Cooper and Mr. Barton Reavis for their help in maintaining and rigging the airplane for the test program.

28940

TABLE OF CONTENTS

SUBJECT	PAGE NUMBERS
List of Tables	3
List of Figures	4-5
Symbols and Conventions	6-8
Aircraft Specifications	9
Summary	10
Introduction	11-12
Instrumentation	13-21
Flight Test Program	22-24
Discussion	25-29
Results	30-33
Conclusions and Recommendations	34-35
Bibliography	36
Calculations	37-42
Tables	43-49
Figures	50-74

LIST OF TABLES

TABLE	PAGE NUMBER
1. Measurement of Weight and Calculation of C.G.	43
2. Frequency Response Data (C.G. = 25.4% M.A.C., V = 140 M.P.H.)	44
3. Frequency Response Data (C.G. = 25.4% M.A.C., V = 100 M.P.H.)	45
4. Frequency Response Data (C.G. = 29.85% M.A.C., V = 140 M.P.H.)	46
5. Frequency Response Data (C.G. = 29.85% M.A.C., V = 100 M.P.H.)	47
6. Frequency Response Data (C.G. = 34.6% M.A.C., V = 140 M.P.H.)	48
7. Frequency Response Data (C.G. = 34.6% M.A.C., V = 100 M.P.H.)	49

LIST OF FIGURES

FIGURE	PAGE NUMBER
1. Test Airplane	50
2. Control Panel and Assembled Instrumentation Components	51
3. SFIM Recorder	52
4. Rate of Turn Gyro Transmitter	52
5. Elevator Oscillating Motor, Wheel, Support, and Drive Shaft	52
6. Rate of Turn Gyro Transmitter Calibration Equipment	53
7. Airplane C.G. Determination Measurements	54
8. Aircraft C.G. Position (% M.A.C.) v.s. C.G. Shifter Weight Counter	55
9. Variation of Stick Fixed Neutral Point and Elevator Power v.s. Lift Coefficient	56
10. Samples of Good SFIM Recorder Film Data	57
11. Samples of Poor SFIM Recorder Film Data	58
12. Normal Acceleration Frequency Response (C.G. = 25.4% M.A.C., V = 140 M.P.H.)	59
13. Pitch Rate Frequency Response (C.G. = 25.4% M.A.C., V = 140 M.P.H.)	60
14. Normal Acceleration Frequency Response (C.G. = 25.4% M.A.C., V = 100 M.P.H.)	61
15. Pitch Rate Frequency Response (C.G. = 25.4% M.A.C., V = 100 M.P.H.)	62
16. Normal Acceleration Frequency Response (C.G. = 29.85% M.A.C., V = 140 M.P.H.)	63
17. Pitch Rate Frequency Response (C.G. = 29.85% M.A.C., V = 140 M.P.H.)	64
18. Normal Acceleration Frequency Response (C.G. = 29.85% M.A.C., V = 100 M.P.H.)	65
19. Pitch Rate Frequency Response (C.G. = 29.85% M.A.C., V = 100 M.P.H.)	66

FIGURE PAGE NUMBER

20. Normal Acceleration Frequency Response (C.G. = 34.6% M.A.C., V = 140 M.P.H.) 67

21. Pitch Rate Frequency Response (C.G. = 34.6% M.A.C., V = 140 M.P.H.) 68

22. Normal Acceleration Frequency Response (C.G. = 34.6% M.A.C., V = 100 M.P.H.) 69

23. Pitch Rate Frequency Response (C.G. = 34.6% M.A.C., V = 100 M.P.H.) 70

24. Calculated and Experimental Normal Acceleration Frequency Response (C.G. = 25.4% M.A.C., V = 140 M.P.H.) 71

25. Calculated and Experimental Pitch Rate Frequency Response (C.G. = 25.4% M.A.C., V = 140 M.P.H.) 72

26. Comparison of Normal Acceleration Linearized Second Order Transfer Function and Experimental Frequency Response (C.G. = 25.4% M.A.C., V = 140 M.P.H.) 73

27. Comparison of Pitch Rate Linearized Second Order Transfer Function and Experimental Frequency Response (C.G. = 25.4% M.A.C., V = 140 M.P.H.) 74

SYMBOLS AND CONVENTIONS

A.R.	aspect ratio $= \frac{b^2}{s}$
C	mean aerodynamic chord (ft.)
C_t	tail mean aerodynamic chord (ft.)
C_e	elevator mean aerodynamic chord (ft.)
C.G.	center of gravity
C_L	lift coeff. $= \frac{L}{qs}$
C_{L_α}	slope of lift curve $= \frac{dC_L}{d\alpha}$
C_{L_δ}	lift coeff. of horizontal tail due to elevator deflection $= \left(\frac{dC_L}{d\delta}\right)_t$
C_{m_α}	stick fixed static stability $= \frac{dC_m}{d\alpha}$
$C_{m_{D\alpha}}$	downwash lag derivative $= \frac{dC_m}{d(D\alpha)}$
$C_{m_{D\theta}}$	damping in pitch derivative $= \frac{dC_m}{d(D\theta)}$
C_{m_δ}	elevator power derivative $= \frac{dC_m}{d\delta}$
D	differential operator with respect to dimensionless time
H_D	density altitude (ft.)
h	non-dimensional inertia about Y axis $= \frac{2}{\mu}\left(\frac{K_Y}{c}\right)^2$
I_Y	moment of inertia of airplane about Y axis (slug ft.^{2})
K_Y	radius of gyration $K_Y{}^2 = \frac{I_Y}{m}$ (ft.)
l_t	tail length (ft.) (dist. from airplane c.g. to a.c. of tail)
m	mass of airplane $= \frac{W}{g}$ (slugs)
M.A.C.	mean aerodynamic chord (ft.)

No	stick fixed neutral point (% M.A.C.)
n_z	normal acceleration - positive up
q	dynamic pressure = $\frac{1}{2}\rho V^2$ (lb. per sq. ft.)
S	wing area (sq. ft.)
S_t	tail area (sq. ft.)
S_e	elevator area (sq. ft.)
T.R.	taper ratio
V	velocity (m.p.h.)
W	gross weight of airplane (lbs.)
$X_{c.g.}$	location of c.g. (% M.A.C.)

GREEK TERMS:

α	angle of attack of wing (degrees)
δ	elevator angle (degrees)
ϵ	downwash angle (degrees)
η_t	tail efficiency factor
ρ	density of air (slugs per cubic ft.)
$\frac{d\epsilon}{d\alpha}$	rate of change of downwash with angle of attack
τ	aerodynamic time = $\frac{m}{\rho sc}$ (sec.)
μ	airplane density factor = $\frac{m}{\rho sc}$
ϕ	phase angle, minus for lag angles (degrees)
ω	angular frequency $(\mathrm{rad.}/_{\mathrm{sec.}})$, or $(\mathrm{rad.}/_{t/\tau})$ if specified

FLIGHT TEST DATA SYMBOLS (Fig. 12-23):

⊙	Flight Test #1
×	Flight Test #2
◬	Flight Test #3
⊡	Flight Test #4
⟐	Flight Test #5
▽	Flight Test #6

AIRCRAFT SPECIFICATIONS

Ryan Navion N5113K

Average Weight as flown	W	=	2825 lbs.
Wing Area	S_w	=	184.2 sq. ft.
Horizontal Tail Area	S_t	=	43 sq. ft.
Elevator Area	S_e	=	15.04 sq. ft.
Aspect Ratio of Wing	A.R.	=	6.04
Aspect Ratio of Tail	A.R.$_t$	=	4.02
Wing Span	b	=	33.38 ft.
Tail Span	b_t	=	13.17 ft.
Wing MAC	C	=	5.7 ft.
Tail MAC	C_t	=	3.34 ft.
Elevator MAC	C_e	=	1.28 ft.
Dist. from c.g. to Tail a.c.	l_t	=	15.04 ft.
Taper Ratio - Wing	T.R.	=	1.83/1
Airplane Inertia, Y axis	I_y	=	3,000 slug ft.^{3}

SUMMARY

The purpose of this investigation was to determine the feasibility of obtaining reliable longitudinal frequency response data for an airplane using simplified techniques, equipment and instrumentation. The particular method involved sinusoidal oscillation of the elevator at various frequencies and measurement of the airplane's response.

The instrumentation was designed and built with the basic premise of simplicity. The elevator was oscillated mechanically, and the response was recorded by a small, lightweight SFIM recording oscillograph. The tests were conducted at two velocities with three different airplane center of gravity locations and the data reduced to general frequency response form. For one of the test cases a comparison was made between the theoretical and experimental response; an analytical expression for the transfer function based on the experimental data was also determined for this case.

This approach proved entirely feasible for obtaining frequency response of the Ryan Navion as repeatable results were obtained with little random error. The same instrumentation scheme could likely be employed in many current production aircraft as the instrumentation space and power requirement is small. This type of testing is however restricted to flight vehicles in which steady state conditions can be achieved.

If stability derivatives are to be obtained from the results of this type investigation, a limitation on the degree of simplicity may be imposed.

INTRODUCTION

Dynamic flight testing of airplanes has until recently been concerned almost completely with the qualitative approach of determining whether the airplane was dynamically stable or unstable. With the growing development in the field of automatically controlled and stabilized aircraft, a quantitative determination of dynamic response characteristics becomes a greater concern. This information is required for the control system designer so that he can consider the airplane with its aerodynamic transfer function as another link in the overall system.

The determination of this transfer function or frequency response for an airplane may be accomplished in a number of ways. First, it could of course be derived analytically, but this introduces all the attendant inaccuracies and difficulties associated with the equations of motion and stability derivatives. A more direct approach is to determine frequency response from either transient or steady state dynamic flight testing. The transient method has the disadvantage of requiring complicated recording instrumentation, and the resulting data is quite difficult to analyze. Its principal advantages result from the economy of flight time required to obtain data, and from the lack of necessity for steady state flight conditions. Steady state dynamic flight testing results in very simple data analysis with the possibility of less complicated instrumentation. It does however require considerably more testing time and steady state conditions are necessary; these demands can limit the applicability of the method.

Longitudinal frequency response data may be obtained for an

airplane through steady state dynamic flight testing utilizing a forcing function upon the airplane's elevator. This forcing function consists of a sinusoidal oscillating elevator input of controllable amplitude and frequency. The frequency response data may then be obtained by recording the airplane's response in normal acceleration, pitch rate, etc. for a steady state condition. The presentation of the frequency response data is accomplished by measuring and plotting vs. frequency the amplitude ratio of that particular function of airplane response desired to the elevator input and the phase angle between them.

Tests of this sort have been conducted by the Cornell Aeronautical Laboratory employing a system utilizing an autopilot with a sine wave generator to give the purest possible sine wave oscillation to the elevator. This led to considerable complication in the instrumentation which made this particular approach impractical for other than scientific types of testing.

This report was conducted to investigate the feasibility of determining frequency response of airplanes by the same type steady state dynamic testing used in the Cornell Aeronautical Laboratory tests. However more simplified instrumentation, applicable to production type airplanes, was used. The system herein discussed involved a mechanical elevator oscillation scheme and the SFIM recorder. The flight tests were conducted in a Ryan Navion at the Forrestal Research Center, Princeton University.

INSTRUMENTATION

General.

Investigation of the frequency response of an aircraft poses two instrumentation problems. First, the aircraft response must be measured and recorded and, second, a sinusoidal elevator excitation must be supplied. In addition, for this thesis simple instrumentation was a primary consideration. The SFIM A-20 flight recorder is an extremely small recording oscillograph that met the above requirements and was selected for use in this investigation. This instrument is a 24 volt D.C. machine, so it was decided that only compatible 24 volt D.C. components would be employed.

The oscillating device was built around a 24 volt surplus antenna reel motor. The choice of where to mount the motor and how to convert the rotary motion to an accurate sinusoidal motion was also dictated by simplicity. A drive shaft and eccentric arm appeared to be the most simple and accurate conversion. Mounting the device in the tail and connecting it directly to the elevator was most desirable but proved impossible because of space limitations, inaccessibility, and safety of flight considerations. Finally, it was decided to mount the unit immediately aft of the front seats with the driving arm extending between the pilot and copilot and connected directly to the base of the control column. This has proven a most satisfactory arrangement.

Components.

The Aircraft. (Fig. 1)

The aircraft used in this investigation was a standard Ryan Navion number N5113K. The only modification to the air-

plane was the addition of a sliding weight mounted along the longitudinal fuselage axis which was used to control the aircraft's center of gravity position. This is described in detail in Princeton Report 275.

Electrical Power Supply.

A 24 volt D.C. two wire system was used. The aircraft's 12 volt battery was connected in series with a second 12 volt heavy duty battery to provide a 24 volt source of power. This power source supplied a bus bar barrier strip mounted on the starboard deck aft of the right rear seat.

SFIM A-20 Flight Recorder. (Fig. 3)

This is a very small (6.5" x 4.75" x 4") ten channel recording oscillograph. Recording of various traces is made on a photographic paper strip by beams of light supplied by the filament of a lamp located in the recorder. This image is projected by mirrors of the measuring instruments which are installed inside the recorder. The recorder incorporates a timing unit which is regulated by a clockwork escapement. Four sockets mounted two on each lateral flange are provided to hold measuring instruments. In this investigation only four channels were utilized, and they recorded elevator deflection, normal acceleration, pitch rate, and time.

The SFIM A-20 flight recorder proved to be a most excellent piece of equipment. The only difficulty experienced in its use was that the film speed of the machine is too slow, approximately 1 ft./min., and this made some high frequency traces difficult to analyze for phase angles. The recorder

holds twenty feet of film which proved to be an adequate amount for each flight.

Normal Accelerometer.

The accelerometer used was a SFIM J531 instrument mounted internally as channel 2 in the recorder. The detecting element is a suspended mass. Range is 0 to 2 g. It is air damped and has a natural frequency of 25 cycles per second. This is well above the range of investigation so no instrument resonance was encountered.

Rate of Turn Gyro Transmitter. (Fig. 4)

The instrument used was a SFIM I 131 rate of turn gyro transmitter. This device transmitted electrically measurements of angular speeds. The measuring element is a 24 volt D.C. gyroscope. The transmitting element is a D.C. potentiometer. Speed of rotation under 27 volts is 9000 RPM. Natural frequency of this component is 5 cycles per second. The range of this investigation is between 0.2 and 0.5 cycles per second, so the dynamic characteristics of this instrument should be accounted for. Range of the instrument is 6°/sec. The instrument is a small cubic box measuring 3.25 inches side length.

The signal transmitted by the potentiometer is received and inscribed on the recording film by a ferromagnetic ratiometer type E 521 mounted internally in the recorder as channel 1.

Elevator Deflection.

The elevator position was measured by a Helipot continuous rotation potentiometer which was located in the tail of

the aircraft. A rigid arm was mounted to the hinge line of the elevator and a string-spring combination used to transmit elevator motion to the potentiometer shaft. The potentiometer was powered by the 24 volt D.C. system and the output signal was received and inscribed on the recording film by a ferromagnetic ratiometer type E 521 mounted internally in the recorder as channel 4.

Oscillating Device. (Fig. 5)

The elevator oscillating device is a very critical item in an investigation of this type. In order to make the flight results of value, the device must drive the elevator sinusoidally at a given frequency and amplitude. Theoretical studies of the airplane's modes of motion indicated that the proper range of frequencies to be investigated was 12 to 150 cycles per minute. Examination of the elevator hinge moments and gearing showed that less than 0.1 HP would be required to deflect the elevator 10 degrees at a "q" of 50 p.s.f. The motor that most nearly met the above requirements at a moderate cost was a surplus 24 volt D.C. antenna reel motor of 1/8 H.P. @ 4000 RPM geared to 150 RPM output. This motor has two field windings for forward and reverse operation. However, in this installation the motor was required to run in only one direction and resourceful utilization of the second field winding provided a built in tachometer generator. The current induced in the second field winding by the armature was measured on an A.C. voltmeter which was used as a tachometer. The motor speed is controlled by a variable

resistance in series with the motor. This resistance consists of a five ohm rheostat and a 3-1/3 ohm resistor which may be added to the circuit by a switch.

The motor is mounted with the shaft parallel to the airplane's lateral axis and drives a small flywheel through a universal joint. The outboard face of the flywheel is drilled and tapped at four radii which represent elevator deflections of approximately 2.5°, 5°, 7.5°, and 10°. Elevator deflection is achieved by mounting a 5/8" grooved pin at the desired radius in the flywheel face. A similar pin is fixed to the base of the control column. A drive shaft connects the flywheel pin and the control column pin and converts the circular motion of the flywheel to the sinusoidal motion at the control column. The ratio of flywheel radius to drive shaft length is less than 1/50 at the maximum elevator deflection. The drive shaft has collars with spring clips on both ends. The spring clips fit into the groove in the pins on the flywheel and control column. The pins are made of mild steel and the collars are made of bronze, hence a proper bearing surface is achieved. In addition the drive shaft incorporates a turnbuckle arrangement for trimming the aircraft and sleeve and setscrew arrangement for gross length adjustment.

The oscillating device is mounted on a 1/4" boiler plate base which is attached to the sliding weight housing immediately aft of the front seats.

Instrument Control Panel. (Fig. 2)

An instrument control panel was mounted on the forward face of the rear seat instrument console. This unit contains an A.C. voltmeter which is used as a tachometer, a D.C. voltmeter for measuring battery potential, the motor rheostat and step resistance, and on-off switches for 24 volt power, SFIM recorder, rate gyro power and signal, and elevator deflection signal. A fast/slow film speed switch was placed in the panel to accommodate both film speeds available in the SFIM recorder. Since only the fast speed of the present recorder was utilized, this switch was left unconnected. In addition, two four-prong receptacles are provided for electrical connections to the SFIM recorder and motor. A three-prong receptacle is provided for electrical connections to the rate gyro. The instrument panel is powered by connections to the 24 volt D.C. bus bar barrier strip which is described above.

Calibration.

Four items required calibration in this instrumentation system. They were the rate gyro, the normal accelerometer, the elevator deflection indicating system, and the tachometer. The aircraft airspeed indicating system was not calibrated because all previous calibrations showed that I.A.S. could be used as C.A.S. with less than 2.0 MPH error for normal aircraft configurations.

The rate of turn gyro was calibrated on a pendulum which consisted of a 3/4" diameter aluminum shaft and a 12" diameter instrument pan. The pendulum was pinned to the overhead truss structure in the

hangar. See Fig. 6. Overall length of the pendulum was 120.75". The rate of turn gyro and the SFIM recorder were mounted on the instrument pan and power was supplied by a 24 volt battery cart through wires which extended down the shaft from the hinge pin to the instruments. Theoretical calculations, based on a pendulum length of 120.75", gave a period of 3.505 seconds. The actual period as determined from the SFIM recorder timer trace was 3.46 seconds. This discrepancy was the result of theoretical calculation based on the overall pendulum length rather than the length to the c.g. of the system. Turn rate was calculated from the relation $\dot{\theta} = \bar{\theta}\omega \cos \omega t$ so that $\dot{\bar{\theta}} = \bar{\theta}\omega$ where ω was actual pendulum frequency and θ was measured angular displacement from zero. Angular displacement was varied in five steps from .083 radians to .1823 radians. The pendulum proved to be isochronous for these amplitudes. Pitch rate gradient was found to be linear and equal to 0.1222 radians/sec. per inch trace amplitude cycle.

The accelerometer was calibrated by securing the SFIM recorder to an adjustable tilt head band saw table. The table angle was measured with a propeller protractor and a record was taken in steps from -70° to +70° tilt. Normal acceleration was calibrated as the cosine of the tilt angle with the zero position equal to 1.0 g. Power for the recorder was supplied by a 24 volt battery cart. Normal acceleration gradient was found to be linear and equal to 0.68 g. per inch trace amplitude cycle.

The elevator deflection was calibrated by measuring elevator deflections between -10° and +10° with a propeller protractor and recording these deflections in one degree steps. For this calibration the SFIM recorder was installed normally in the aircraft instrumenta-

tion system and powered by the 24 volt D.C. power source. The elevator deflection gradient was found to be non-linear at the extreme deflections, but was linear within a 5° deflection range about the required elevator trim position. The gradient was found to be 5.97 degrees per inch trace amplitude cycle.

The tachometer was calibrated in flight by timing the motor RPM at various resistance settings and then assigning RPM values to measured induced voltage readings on the A.C. voltmeter. Accuracy of the tachometer system allowed only order of magnitude readings, but this reading proved to be of great value in the flight test program. The actual frequencies were determined later from the SFIM recorder timer record.

Instrumentation Deficiencies.

Experience uncovered two rather serious deficiencies in the instrumentation system. The first of these was the speed of film travel in the SFIM recorder. Two speeds are available in this model, 1 mm/sec and 5 mm/sec. Although the faster speed was employed throughout the investigation, considerable difficulty was experienced in obtaining phase angles at high frequencies. Low frequency phase angles could be found with some accuracy, but it is felt that high frequency results are unreliable due to difficulty in data reduction. This film speed defect created no amplitude measurement problems however, and amplitude response is considered satisfactory. Unfortunately, there was no method of increasing film speed in this recorder and this shortcoming remainded uncorrected.

The second deficiency was in the oscillating device. Unfort-

unately, motor torque varied directly with voltage, and while the motor could be made to run slowly, it produced too little torque to operate the oscillating system. This inadequacy was eliminated by the addition of a 4.5:1 reduction gear and a second drive shaft. Two mounting positions for the motor were established so that the oscillating device could be driven by either the low or high speed shaft. The shaft connection can be changed in approximately 15 minutes. No further difficulty was experienced with this problem.

A third, rather disconcerting defect was discovered on the initial shakedown flight when the oscillating device was being tested. The spring clip releases on both front and rear collars of the drive shaft linkage were designed as quick release devices and had been satisfactorily tested on the ground. They did not work in the air however, and the airplane, instrumentation, and authors were very nearly destroyed before manual control could be restored. After this experience a T handle set screw arrangement was incorporated in the drive shaft linkage. See Fig. 5. This proved to be of aid in starting the oscillations in addition to giving peace of mind as an overall safety device.

FLIGHT TEST PROGRAM

The flight test program was designed to obtain data for six flight conditions at 5000 feet density altitude. These flight conditions were for two airspeeds, 100 MPH and 140 MPH, at three center of gravity positions; 25.40, 29.85, and 34.60% m.a.c. As experience was gained in data recording procedure, the 20 minute film duration of the SFIM recorder proved to be sufficient time to investigate all six of these conditions on each flight. Due to the change in motor installation required to investigate the entire frequency range, it was decided that only one frequency range should be investigated on any flight. Low frequency data was obtained first and after sufficient repeatable results were obtained the motor was remounted and the test program repeated to obtain high frequency data.

Each flight test crew consisted of a pilot and a copilot-recorder, and the following procedure was adhered to on each flight. Prior to take off the power source was checked for a 25 volt minimum indication and the instrumentation system was tested. While climbing to 5000 ft. density altitude the rate of turn gyro was uncaged, the sliding weight was shifted to obtain the desired c.g. location, the instrument check list completed, and the drive shaft linkage connected with the set screw unlocked so that the pilot retained normal control of the aircraft. When at altitude the pilot adjusted power and elevator trim tab for steady level flight in the desired flight condition. With the drive linkage still unlocked the copilot turned on and adjusted the speed of the oscillating device. The pilot then locked the set screw on the drive shaft linkage thereby completing the connection

from the device to the elevator. It was necessary for the pilot to lock on in a position that caused the elevator to be oscillated about the elevator trim deflection, otherwise a somewhat uncomfortable nose-up or nose-down trend accompanied the normal oscillation. A satisfactory lock on usually required several attempts. After the gross adjustment had been achieved by a satisfactory lock on, airspeed and altitude were observed and final adjustments accomplished by the turnbuckle linkage trim system. Patience was required in this process but skill was acquired with experience. After all adjustments were completed, the copilot turned on the recorder and at least ten steady state cycles were recorded. The recorder was then turned off and the linkage unlocked. The copilot made an entry in the data log of airspeed, altitude, tachometer reading, and any additional pertinent comments. He then set the rheostat for a different frequency and the lock on and recording procedure was repeated until all desired frequencies in that condition were investigated. A new condition was then effected by changing the c.g. location or airspeed. The most efficient method of covering all conditions was determined to be to start the runs at 100 MPH in the aft c.g. condition, then go to 140 MPH at the same c.g. location, next to shift to mid c.g. while maintaining 140 MPH, etc. with the final run made at 140 MPH with c.g. forward. At the completion of the tests, the rate tyro was caged and the instruments secured.

Flights 1 through 4 were investigations in the low frequency range. After flight 4 the motor was remounted and flights 5 and 6 were investigations in the high frequency range. On flight 1, a 5/8" foam rubber pad was placed under the SFIM recorder and the rate gyro.

This was done to eliminate trace distortion due to airframe vibrations. On flight 2 the sponge was removed and both flight records were studied. There appeared to be no vibration distortion in the flight 2 record so the sponge pad was not used on subsequent flights. In addition, it is felt that some inaccuracy may result in the normal acceleration record due to the cushioning effect of the foam rubber pad if it is used.

Rough air makes this type testing prohibitively difficult. Moderate turbulence was found to continuously excite the phugoid mode, as evidenced by slow altitude and airspeed oscillations, which required constant trim change to control. Flights 4 and 5 were recorded at 5500 ft. density altitude in order to avoid turbulence at the 5000 ft. level at the time of the tests.

Of interest to individuals involved in this type of flight test program is the physical discomfort which may be experienced. The authors found that the person acting as recorder is strongly affected by nausea, particularly at the short period resonance frequency, while the person actually in control of the aircraft is affected but little. This leads to the interesting supposition that man is sensitive to third and fourth displacement derivatives with respect to time.

DISCUSSION

The utilization of frequency response data for an airplane has been discussed in the introduction. The primary purpose of this investigation was to determine the feasibility of obtaining reliable longitudinal frequency response data from steady state dynamic flight testing employing simplified instrumentation. With simplicity as a primary goal, it was decided to supply a longitudinal forcing function to the airplane consisting of a mechanically induced sinusoidal elevator deflection of controllable amplitude and frequency. The SFIM recorder provided a lightweight, simplified means of recording this elevator input and the airplane's steady state response in normal acceleration and pitch rate. Angle of attack response may be obtained from normal acceleration response.

Since the test airplane had a sliding weight installed, it was decided to conduct the flight tests at 3 separate C.G. locations in order to observe the effect of static stability on the longitudinal frequency response. The airplane was weighed in the flight test configuration while moving the sliding weight through its entire range. This enabled a calibration for the airplane C.G. (% M.A.C.) vs. the sliding weight position counter. See Table 1 and Figs. 7 and 8. The flight tests were run with the counter readings 0000, 9900, and 9794 which gave C.G. positions of 25.4, 29.85 and 34.6% M.A.C. respectively.

In order to observe the effect of flight velocity on frequency response, it was decided to conduct the flight tests at two true air speeds for each C.G. location. The true air speeds used were 100 and 140 M.P.H. The flight tests were conducted at a density altitude of 5000 feet.

In designing the instrumentation system, it was necessary to predict the results which could be expected. This enabled an estimation of the magnitudes and frequencies of elevator oscillation required and the approximate mechanical power necessary to drive the system. The estimated values of expected pitch rate, normal acceleration, and elevator deflection were also necessary so that required capabilities of the recording components could be determined.

In calculating the longitudinal frequency response, it was necessary to determine the range of oscillation frequencies required. Examination of previous tests of this nature indicated that these frequencies should include the span from approximately 12 to 150 cycles per minute. For the flight test configurations to be used, it was estimated that the period of the phugoid mode would vary from approximately 20 to 30 seconds. Since the period of the minimum excitation frequency was 5 seconds, it was assumed that little forcing of the phugoid mode would be encountered.

The assumption of negligible excitation of the phugoid mode permitted consideration of the steady state flight tests at constant velocity. The linearized, longitudinal equations of motion could therefore be simplified by eliminating the entire drag equation and velocity terms from the lift and pitching moment equations. The latter two equations give a simplified solution for the response of the short period mode.

Using these equations, the frequency response for normal acceleration and pitch rate was calculated as outlined in the calculations section of this report. The flight test condition of C.G. at

25.4% M.A.C. and V = 140 m.p.h. was selected as representative of an average level of response for the various flight conditions. The stability derivatives for the airplane were calculated and compared with those obtained experimentally in previous reports. The values considered most reliable were used in the calculations, and their values and source are shown in the calculation section. The values for stick fixed neutral point and elevator power were taken from Princeton Aeronautical Engineering Report No. 275, and are functions of lift coefficient. They are plotted in this report as Fig. 9. If it were desired to calculate the frequency response for other flight conditions, Xc.g. could be obtained from Fig. 8, and N_0 and C_{m_δ} from Fig. 9. The same procedure used in the example solution could then be followed assuming that the other derivatives are invariant with flight condition.

The instrumentation system previously discussed was designed using the results of the calculations. A comparison of the calculated and experimentally obtained frequency response data for the particular flight condition described above is given in Figs. 24 and 25. Although there was a sizeable discrepancy, it was extremely gratifying to the authors that the original instrumentation design proved completely adequate throughout the entire flight test range. The capabilities of the recording elements were properly utilized and their limits were never exceeded. As previously mentioned, a faster film speed for the SFIM recorder was highly desirable in order to obtain more accurate phase angle determination, but this was beyond the authors' control. The deficiencies encountered in the elevator oscillating system were quickly remedied. It is felt that this simplified instrumentation

system will yield reliable longitudinal frequency response data and is relatively trouble free.

Samples of flight test data are contained in Figs. 10 and 11. The method used for data reduction may be explained by reference to the samples of good data contained in Fig. 10. For a particular frequency of elevator oscillation, the frequency was obtained by taking 5 cycles of the purest sinusoidal traces. The dashed lines at the bottom of the film are from the SFIM recorder timer and represent 1 second intervals. With dividers the length of 5 cycles was laid off on the time scale such that the time in seconds for 5 cycles was measured. Angular frequency in radians/sec. was then obtained by multiplying 5 by 2π and dividing by the time in seconds. The amplitude ratios were obtained by summing the amplitudes over 5 cycles of each trace with dividers. The summations were measured with a 60 graduations/inch scale. The summation for normal acceleration and pitch rate was then divided by the summation for elevator deflection. For phase angle measurement the length of five cycles was measured on the scale. Then the phase angles between the normal acceleration and elevator traces and between the pitch rate and elevator traces were summed over 5 cycles and measured on the scale. The particular phase angle was then the ratio of phase angle sum to 5 cycles sum multiplied by 360°. The inadequacy of phase angle measurement at the higher frequencies is readily apparent from observing the distance represented by one cycle or 360° of trace.

Some examples of poor data are contained in Fig. 11. In each case of poor data, it was readily apparent to the pilots conducting the tests and noted on the flight data sheet. In film A, rough air

was encountered. As mentioned in the flight test section of this report, on the flight encountering rough air, further tests were conducted at 5,500 feet density altitude. In film B, an example of the presence of the phugoid mode may be seen. It was observed during the flight tests that occasional gusts and appreciable trim changes would excite the phugoid mode. This was evidenced by slow deviations in air speed and altitude, and whenever encountered, further flight tests were conducted. It is interesting to note that the normal air speed variation during the tests was of the order of ± 2 m.p.h. which would tend to substantiate the constant velocity assumption. In film C, an example of erratic pitch rate response may be observed. This resulted from an experiment with the mounting support of the rate of turn gyro transmitter. In this case the gyro was directly mounted on the boiler plate without its usual hard rubber pad. In film D, an example of elevator distortion may be seen. This resulted from overloading the motor by using excessively large elevator displacements. Elevator distortion was also present at the lower frequencies before the elevator driving motor was geared down. This was due to the motor being overloaded for its driving voltage and the results were an obviously non-sinusoidal elevator input.

RESULTS

The frequency response curves of $\frac{n_z}{\delta}$ and $\frac{\dot{\theta}}{\delta}$ were obtained for six flight conditions and are shown on Figures 12 through 23. It should be noted that these plots have abscissas in real time, radians/sec., rather than aerodynamic time, radians$/_{t/\tau}$. The ordinates of the pitch rate curves are also in real rather than aerodynamic time. In addition, the ordinates of the normal acceleration curve must be corrected to radian measure if stability derivatives are to be investigated.

These frequency response curves are a graphical representation of the normal acceleration and pitch rate transfer functions of the Ryan Navion. Figures 24 and 25 compare experimental and theoretical frequency response curves for the 140 MPH, 25.4% m.a.c. flight condition. To better understand these results, an analytical expression for the experimental results was found by a curve fitting process. The airplane was assumed to have a linear second order characteristic equation, $D^2 + bD + k = 0$. The normal acceleration transfer function, neglecting tail lift, is then of the form $\frac{C}{S^2 + bS + k}$. These constants are easily evaluated from plots of amplitude and phase response of a second order sinusoidally forced system.

$$\ddot{\theta} + 2\zeta\omega_n\dot{\theta} + \omega_n^2 = F\sin\omega t$$

These plots may be found in any dynamics textbook. The method employed to evaluate these constants was an iterative process of selecting a trial ω_n, finding the gain constant C for this ω_n, then making a ζ search until the best fit was obtained. From this ζ a new ω_n was selected and the cycle repeated. An excellent curve fit was obtained for the normal acceleration amplitude ratio from the use of

$\omega_n = 5.5$, $\zeta = 0.8$, and $C = 0.258$. A proper curve fit of amplitude ratio rather than phase angle was chosen because of previously discussed difficulties encountered in reducing phase data. The analytic expression for the experimental normal acceleration transfer function is then $\frac{n_z}{\delta} = \frac{0.258}{S^2 + 8.8S + 30.3}$ in real time, or $\frac{n_z}{\delta} = \frac{0.200}{S^2 + 7.75S + 23.5}$ in aerodynamic time.

The pitch rate transfer function, neglecting tail lift, is then of the form $\frac{C\ (A + Bs)}{S^2 + bS + k}$ which may be written $\frac{\dot{\theta}}{\delta} = \frac{n_z}{\delta}(A + Bs)$.

The constants A and B were found by the slope intercept method from a plot of $\left(\frac{\dot{\theta}/\delta}{n_z/\delta}\right)$ versus frequency. The analytic expression for the experimental transfer function is then $\frac{\dot{\theta}}{\delta} = \frac{0.258\ (6.0 + 2.0s)}{S^2 + 8.8S + 30.3}$ in real time, or $\frac{D\theta}{\delta} = \frac{0.227\ (5.29 + 2.0s)}{S^2 + 7.75S + 23.5}$ in aerodynamic time. Results of these analytic expressions are compared to the experimental curves in Figures 27 and 28. With the exception of the pitch rate phase angle, the airplane appears to be well represented by these second order analytic expressions in the frequency range investigated. Higher frequency results indicate there may be some higher order effects not accounted for.

The value of the constants b, K, C, A, and B in the experimental transfer functions are considerably different than calculated theoretical values. In addition, a preliminary analysis of stability derivatives as determined from experimental data gives some unrealistic results. Possible sources of error were then considered.

Repeatability of data eliminates random error as a source. Faulty assumptions in the theoretical analysis appear unlikely since proper altitudes, air speed, and steady state conditions were achieved during the flight tests. Stability derivatives used in the theoretical analysis may be a source of error. The static stability derivative used in the analysis was obtained from the one "g" flight condition and may be quite different from the required $(C_{m_\alpha})_{V=K}$ value. Another source of error could be in the sinusoidal forcing function since no harmonic analysis was made. However, examination of the elevator trace indicates any error of this type would be very small.

The possibility of system error in the instrumentation was then considered. An error in pitch rate response was found to have been introduced by the rate gyro. The frequency response of the rate gyro was not considered in the calibration of this instrument, and hence proper corrections to rate gyro response were not made in the reduction of flight test data. It had been assumed that since the rate gyro has a natural frequency of 5 c.p.s. no resonance in the response of the gyro would be experienced. This was probably a valid assumption since the gyro probably has a standard damping factor of 0.7. While this would create no error in amplitude ratio response, a considerable additional lag due to the gyro is added to the pitch rate response. For example, at a forcing frequency of 10 radians/sec. there is a gyro lag error of 27° introduced in the pitch rate phase angle response. This error accounts for the discrepancy between the analytic expression of the transfer function and the experimental curves as seen in Figure 27. In addition, re-examination of the rate gyro calibration revealed

a slightly non linear amplitude characteristic. As much as 10% error in pitch rate amplitude could have been introduced due to this non-linearity. Other system errors may exist but, if so, they were not discovered.

A major difference in theoretical response and experimental response is seen in the characteristic equation. This is not affected by the above rate gyro errors. The aerodynamic spring constant k, was determined by ω_n from the normal acceleration response and is felt to be accurate. This term is $k \doteq (C_{m_\alpha} + \frac{C_{L_\alpha}}{2} \quad C_{m_{D\theta}})$ and considerable difference must consequently exist between these actual stability derivatives and the values used for the derivatives in the theoretical analysis. Quantitative isolation of this difference is felt to be beyond the scope of this report but appears to be a worthy subject of future investigation.

CONCLUSIONS AND RECOMMENDATIONS

The method herein discussed for obtaining longitudinal frequency response is entirely feasible in most conventional type airplanes. The method does, however, have certain inherent disadvantages: the most important are as follows:

1. Even though the elevator oscillation system used in this investigation was uncomplicated, a certain amount of space and rigging was required. This may make the system impractical or impossible in many types of airplanes.
2. The recording instrumentation must have a high degree of accuracy.
3. Smooth flight conditions must prevail.
4. The method requires considerable flight time.
5. The tests are quite uncomfortable for the pilots.

In this investigation the data proved to be very repeatable indicating little random error. However, the lack of agreement between experimental and theoretical results indicates an instrumentation system error and/or a discrepancy in the theoretical and actual stability derivatives must exist. The error in the pitch rate phase angle due to rate gyro dynamic characteristics is such a system error. The lack of correlation between experimental and theoretical characteristic equations strongly indicates that the latter error may also exist.

For further investigations of this type, it is recommended that more careful calibration of the instrumentation be made. Particular emphasis should be on the pitch rate gyro to insure, first, that it is linear in the desired range and, second, that the gyro frequency

response characteristics be known. It is also recommended that a recorder with a higher film speed be used so that accurate phase angles can be obtained.

It is considered that this system is completely adequate for further investigation of frequency response and for frequency response methods of obtaining stability derivatives. It is recommended that further tests be made to positively account for the discrepancy between the theoretical and experimental results presented here.

BIBLIOGRAPHY

1. Airplane Performance, Stability and Control, by Perkins, Courtland D.; and Hage, Robert E.; New York: John Wiley & Sons, Inc., 1949.

2. Advisory Group for Aeronautical Research and Development Flight Test Manual, Volume II, Stability and Control, Edited by Perkins, Courtland D.

3. Advisory Group for Aeronautical Research and Development Flight Test Manual, Volume III, Instrumentation Catalogue, Edited by Perkins, Courtland D.

4. Societe De Fabrication D'Instruments De Mesure, Technical Information, SFIM, 140 rue La Fayette, Paris, France.

5. Princeton University Aero. Eng. Report No. 231, "Determination of Airplane Longitudinal Stability Derivatives from Transient Responses," by Cooley, Petersen, and Irvine; 1953.

6. Princeton University Aero. Eng. Report No. 232, "Determination of Longitudinal Stability Parameters by Steady State Flight Testing and Theoretical Calculations for the Ryan Navion," by Schuld, Emil P.; and Reinhart, Leonard J.; 1953.

7. Princeton University Aero. Eng. Report No. 275, "An Analysis of Various Methods of Flight Testing for Neutral Points," by Matsen, Ralph S.; and Spillers, Willum H.; 1955.

CALCULATIONS

Theoretical approximation to longitudinal frequency response:

The forcing function used is a mechanically introduced sinusoidal elevator deflection of controllable amplitude and frequency:

$$\delta_e = \delta_0 \sin \omega t$$

The frequency of elevator oscillation, ω , will be varied to obtain the amplitude and phase angle frequency response for normal acceleration and pitch rate. It is assumed that ω will be kept sufficiently high, such that any excitation of the airplane's phugoid mode will be negligible. This permits the assumption that V = constant. The standard, linearized, longitudinal equations of motion may then be simplified as follows for considering only the airplane's short period longitudinal response:

Lift eq. $$\left(\frac{C_{L\alpha}}{2} + D\right)\alpha \quad - D\theta \quad = -\frac{C_{L\delta}}{2}\delta$$

Pitching Mom. eq. $$\left(C_{m_\alpha} + C_{m_{D\alpha}} D\right)\alpha \quad + \left(C_{m_{D\theta}} - hD\right)D\theta \quad = -C_{m_\delta}\,\delta$$

Normal Acceleration Response:

$$\alpha = \frac{\begin{vmatrix} -\frac{C_{L\delta}}{2}\delta & -1 \\ -C_{m_\delta}\delta & (C_{m_{D\theta}} - hD) \end{vmatrix}}{\begin{vmatrix} \left(\frac{C_{L\alpha}}{2} + D\right) & -1 \\ (C_{m_\alpha} + C_{m_{D\alpha}} D) & (C_{m_{D\theta}} - hD) \end{vmatrix}} \qquad \text{and} \qquad \frac{C_{L\delta}}{2} = -\frac{C_{m_\delta}}{2\ell_t/c}$$

$$\therefore \quad \alpha = \frac{\left[-C_{m_\delta} + \frac{C_{m_\delta}}{2\ell_t/c}(C_{m_{D\theta}} - hD)\right]\delta}{-hD^2 + \left(-\frac{C_{L\alpha}}{2}h + C_{m_{D\alpha}} + C_{m_{D\theta}}\right)D + \left(C_{m_\alpha} + \frac{C_{L\alpha}}{2}C_{m_{D\theta}}\right)}$$

Let: $$b = \left(-\frac{C_{L\alpha}}{2} h + C_{m_{D\alpha}} + C_{m_{D\theta}}\right)$$

$$K = \left(C_{m\alpha} + \frac{C_{L\alpha}}{2} C_{m_{D\theta}}\right)$$

$$\therefore \quad \frac{\alpha}{\delta} = \frac{-C_{m_\delta}\left[1 - \frac{1}{2\ell_\tau/c}\left(C_{m_{D\theta}} - hD\right)\right]}{-hD^2 + bD + K}$$

To determine the amplitude ratio and frequency response, consider $\vec{\alpha}$ and $\vec{\delta}$ as rotating vectors. Substitute $D = i\omega$ into the equations: (ω in radians$/_{t/\tau}$)

$$\frac{\vec{\alpha}}{\vec{\delta}} = \frac{-C_{m_\delta}\left[\left(1 - \frac{C_{m_{D\theta}}}{2\ell_\tau/c}\right) + \left(\frac{h\omega}{2\ell_\tau/c}\right) i\right]}{\left(K + h\omega^2\right) + (b\omega) i}$$

$$\frac{\vec{\alpha}}{\vec{\delta}} = \frac{-C_{m_\delta}\sqrt{\left(1 - \frac{C_{m_{D\theta}}}{2\ell_\tau/c}\right)^2 + \left(\frac{h\omega}{2\ell_\tau/c}\right)^2} \;\; \angle \tan^{-1} \frac{\left(\frac{h\omega}{2\ell_\tau/c}\right)}{\left(1 - \frac{C_{m_{D\theta}}}{2\ell_\tau/c}\right)}}{\sqrt{b^2\omega^2 + \left(K + h\omega^2\right)^2} \;\; \angle \tan^{-1}\left(\frac{b\omega}{K + h\omega^2}\right)}$$

For the case where $\left(\frac{C_{m_{D\theta}}}{2\ell_\tau/c}\right) \ll 1$ and $\left(\frac{h\omega}{2\ell_\tau/c}\right)^2 \ll 1$ the above eq. reduces to: (For example case this applied)

$$\frac{\vec{\alpha}}{\vec{\delta}} = \frac{-C_{m_\delta}}{\sqrt{b^2\omega^2 + \left(K + h\omega^2\right)^2}} \;\; \angle \tan^{-1}\left(\frac{h\omega}{2\ell_\tau/c}\right) - \angle \tan^{-1}\left(\frac{b\omega}{K + h\omega^2}\right)$$

To convert the above ratio $\frac{\vec{\alpha}}{\vec{\delta}}$ to $\frac{\vec{n}_z}{\vec{\delta}}$ the lift equation on the preceding page can be reduced in the following manner:

$$\frac{C_{L\alpha}}{2}\alpha + (D\alpha - D\theta) - \frac{C_{m\delta}}{2\,l_t/c}\delta = 0$$

$(D\alpha - D\theta)$ = non dimensional centrifugal force = $-\frac{C_L}{2} n_z$.

n_z = incremental load factor positive up = (bad factor -1). Again consider $\vec{\alpha}$ and $\vec{\delta}$ as rotating vectors and the equation becomes:

$$\frac{C_{L\alpha}}{2}\frac{\vec{\alpha}}{\vec{\delta}} - \frac{C_L}{2}\frac{\vec{n}_z}{\vec{\delta}} - \frac{C_{m\delta}}{2\,l_t/c} = 0$$

$$\therefore \frac{\vec{n}_z}{\vec{\delta}} = \left(\frac{C_{L\alpha}}{C_L}\frac{\vec{\alpha}}{\vec{\delta}} - \frac{C_{m\delta}}{C_L\cdot l_t/c}\right)$$

$$\text{or} \quad \frac{\vec{n}_z}{\vec{\delta}} = \frac{-\frac{C_{m\delta}C_{L\alpha}}{C_L}}{\sqrt{b^2\omega^2 + (K+h\omega^2)^2}} \angle\tan^{-1}\left(\frac{h\omega}{2\,l_t/c}\right) - \angle\tan^{-1}\left(\frac{b\omega}{K+h\omega^2}\right) - \frac{C_{m\delta}}{C_L\cdot l_t/c}$$

The above equation will give the amplitude ratio and phase angle for $\frac{n_z}{\delta}$. The correction factor $\left(\frac{C_{m\delta}}{C_L\cdot l_t/c}\right)$ must be added vectorially; in this case, this is a significant factor and must be included.

Pitch Rate Response: (Use the same procedure as before)

$$D\theta = \frac{\begin{vmatrix} \left(\frac{C_{L\alpha}}{2}+D\right) & -\frac{C_{L\delta}}{2}\delta \\ (C_{m_\alpha}+C_{m_{D\alpha}}D) & -C_{m_\delta}\delta \end{vmatrix}}{\begin{vmatrix} \left(\frac{C_{L\alpha}}{2}+D\right) & -1 \\ (C_{m_\alpha}+C_{m_{D\alpha}}D) & (C_{m_{D\theta}}-hD) \end{vmatrix}} = \frac{-C_{m_\delta}\delta\left(\frac{C_{L\alpha}}{2}+D\right)-\frac{C_{m_\delta}}{2\ell_t/c}\delta\left(C_{m_\alpha}+C_{m_{D\alpha}}D\right)}{-hD^2+bD+K}$$

$$\frac{D\theta}{\delta} = \frac{-C_{m_\delta}\left[\left(\frac{C_{L\alpha}}{2}+\frac{C_{m_\alpha}}{2\ell_t/c}\right)+\left(1+\frac{C_{m_{D\alpha}}}{2\ell_t/c}\right)D\right]}{-hD^2+bD+K}$$

$$\frac{\overrightarrow{D\theta}}{\overrightarrow{\delta}} = \frac{-C_{m_\delta}\sqrt{\left(\frac{C_{L\alpha}}{2}+\frac{C_{m_\alpha}}{2\ell_t/c}\right)^2+\left(1+\frac{C_{m_{D\alpha}}}{2\ell_t/c}\right)^2\omega^2}}{\sqrt{b^2\omega^2+(K+h\omega^2)^2}} \; \frac{\angle \tan^{-1}\dfrac{\left(1+\frac{C_{m_{D\alpha}}}{2\ell_t/c}\right)\omega}{\left(\frac{C_{L\alpha}}{2}+\frac{C_{m_\alpha}}{2\ell_t/c}\right)}}{\angle \tan^{-1}\left(\dfrac{b\omega}{K+h\omega^2}\right)}$$

For this airplane $\left(\frac{C_{m_\alpha}}{2\ell_t/c}\right) \ll \frac{C_{L\alpha}}{2}$ and $\left(\frac{C_{m_{D\alpha}}}{2\ell_t/c}\right) \ll 1$; therefore, the equation can be simplified to the following :

$$\frac{\overrightarrow{D\theta}}{\overrightarrow{\delta}} = \frac{-C_{m_\delta}\sqrt{\left(\frac{C_{L\alpha}}{2}\right)^2+\omega^2}}{\sqrt{b^2\omega^2+(K+h\omega^2)^2}} \; \angle \tan^{-1}\left(\frac{2\omega}{C_{L\alpha}}\right) - \angle \tan^{-1}\left(\frac{b\omega}{K+h\omega^2}\right)$$

$$\frac{\overrightarrow{\theta}}{\overrightarrow{\delta}} = \frac{1}{\tau} \cdot \frac{\overrightarrow{D\theta}}{\overrightarrow{\delta}}$$

Example Solution:

$V = 140 \text{ mph} = 205 \text{ ft/sec}$

$X_{c.g.} = 0.254\%$ M.A.C. (Counter at 0000. See Fig. 8)

$H_D = 5000 \text{ feet}$

$$C_L = \frac{2 \text{ Wave.}}{\rho SV^2} = \frac{2(2825)}{(.00205)(184.2)(205)^2} = 0.356$$

$N_o = 0.364$ (Neutral point % M.A.C.) (See Fig. 9)

$$\frac{l_t}{c} = \frac{15.04}{5.7} = 2.64$$

$$m = \frac{\text{Wave.}}{g} = \frac{2825}{32.2} = 87.8 \text{ slugs}$$

$$\tau = \frac{m}{\rho SV} = \frac{87.8}{(.00205)(184.2(205)} = 1.135 \text{ sec}$$

$$\mu = \frac{m}{\rho SV} = \frac{87.8}{(.00205)(184.2)(5.7)} = 40.8$$

$I_y = 3{,}000 \text{ slug ft}^2$ (An approximation from Princeton Aeronautical Engineering Report No. 231)

$$K_y^2 = \frac{I_y}{m} = \frac{3{,}000}{87.8} = 34.2 \text{ ft}^2$$

$$h = \frac{2}{\mu}\left(\frac{K_y}{c}\right)^2 = \frac{2\ (34.2)}{40.8\ (5.7)^2} = 0.0515$$

$C_{L_\alpha} = 4.81$ (Princeton Aeronautical Engineering Report No. 231)

$$\left.\begin{aligned} C_{m_{D\alpha}} &= -0.08 \\ C_{m_{D\theta}} &= -0.17 \end{aligned}\right\} \text{Theoretical valves}$$

$$C_{m_\alpha} = C_{L_\alpha}(X_{cg} - N_o) = 4.81\,(.254 - .364) = -0.53$$

$C_{m_\delta} = -.01785$ per degree (See Fig. 9)

$$b = \left(\frac{-C_{L_\alpha}}{2}h + C_m + C_{m_{D\theta}}\right) = -\frac{4.81}{2}(.0515) - 0.08 - 0.17 = -0.3$$

$$k = \left(C_{m_\alpha} + \frac{C_{L_\alpha}}{2} C_{m_{D\theta}}\right) = -0.53 - \frac{4.81}{2}(0.17) = -0.940$$

$$\frac{C_{m_\delta} C_{L_\alpha}}{C_L} = \left(\frac{-.01785}{.356}\right) 4.81 = -0.237$$

$$\frac{C_{m_\delta}}{C_L\, l_t/c} = \left(\frac{-.01785}{.356}\right)\left(\frac{1}{2.64}\right) = -.0190$$

$$\frac{\vec{n_z}}{\vec{\delta}} = \frac{0.237}{\sqrt{(0.374)^2\omega^2 + (-.940+.0515\omega^2)^2}} \angle \tan^{-1}\left(\frac{.0515\omega}{5.28}\right) - \angle \tan^{-1}\left(\frac{-.374\omega}{-.940+.0515\omega^2}\right) + .0$$

$$\frac{\vec{n_z}}{\vec{\delta}} = \frac{4.67}{\sqrt{\omega^4 + 16.2\omega^2 + 333}} \angle \tan^{-1} 0.00975\omega - \angle \tan^{-1}\left(\frac{7.27\omega}{18.3-\omega^2}\right) + 0.019$$

$$\frac{\vec{\dot{\theta}}}{\vec{\delta}} = \frac{17.5\sqrt{5.78+\omega^2}}{\sqrt{\omega^4+16.2\omega^2+333}} \angle \tan^{-1}\left(\frac{\omega}{2.40}\right) - \angle \tan^{-1}\left(\frac{7.27\omega}{18.3-\omega^2}\right)$$

These calculated plots are shown in Figures 24 and 25 and are compared to the test data for this case.

TABLE 1

Measurement of Weight and Calculation of Center of Gravity

Conditions:

1. Landing gear retracted, flaps up.
2. Full gas load.
3. Canopy closed.
4. Two pilots with parachutes in forward seats.
5. Additional 12-volt battery in aft compartment.
6. C.G. shifter weight installed.
7. Thesis instrumentation in the airplane.

Measurements:

C.G. Indicator	Weight Forward	Weight Aft	Total Weight	Dist. of C.G. aft of Jack Pts.	Dist. of C.G. aft of o% MAC	C.G. % MAC
0000 Full Forward	2705	140.5	2845	11.16	16.46	25.4
9930	2680	165.5	2845	13.14	18.44	28.5
9860	2654	191.3	2845	15.20	20.50	31.6
9794 Full Aft	2630	215.0	2845	17.09	22.40	34.6

TABLE 2

Flight Condition

C.G. = 25.4% M.A.C.
V = 140 MPH
H_D = 5,000 Ft

Flight #	ω (rad/sec)	$\frac{\lvert n_z \rvert}{\lvert \delta \rvert}$	$\phi_{n_z \delta}$	$\frac{\lvert \dot{\theta} \rvert}{\lvert \delta \rvert}$	$\phi_{\dot{\theta} \delta}$
1	4.27	0.201	-257°	2.93	-206°
1	3.38	0.216	-247°	2.88	-195°
1	2.20	0.235	-227°	2.52	-180°
1	1.48	0.253	-217°	2.44	-180°
1	1.19	0.260	-204°	2.03	-180°
3	4.89	0.167	-270°	2.95	-221°
3	4.13	0.195	-258°	2.99	-207°
3	3.27	0.226	-240°	2.91	-198°
3	2.13	0.254	-220°	2.55	-180°
4	4.94	0.181	-272°	3.05	-215°
4	4.05	0.203	-262°	3.06	-200°
4	3.19	0.225	-248°	2.79	-190°
4	2.06	0.251	-230°	2.51	-
4	1.21	0.256	-205°	2.19	-
5	16.31	0.045	-	1.00	-
5	13.62	0.051	-	1.16	-
5	11.62	0.062	-320°	1.41	-
5	7.85	0.097	-298°	2.14	-255°
5	5.71	0.160	-284°	2.65	-223°
6	18.46	0.038	-	0.63	-
6	13.94	0.052	-	1.14	-
6	12.56	0.059	-	1.45	-
6	10.68	0.074	-	1.64	-
6	10.05	0.081	-320°	1.75	-265°
6	8.05	0.100	-310°	2.13	-250°
6	7.23	0.114	-300°	2.36	-240°
6	4.76	0.174	-274°	2.89	-213°

TABLE 3

Flight Condition

C.G. = 25.4% M.A.C.
V = 100 MPH
H_D = 5,000 Ft

Flight #	ω (rad./sec.)	$\frac{\lvert n_z \rvert}{\lvert \delta \rvert}$	$\phi_{n_z \delta}$	$\frac{\lvert \dot{\theta} \rvert}{\lvert \delta \rvert}$	$\phi_{\dot{\theta} \delta}$
1	4.61	0.066	-281°	1.64	-218°
1	4.24	0.070	-278°	1.72	-216°
1	3.74	0.081	-273°	1.75	-213°
1	3.23	0.088	-268°	1.74	-206°
1	2.96	0.090	-261°	1.73	-203°
1	2.25	0.102	-240°	1.61	-190°
1	1.46	0.115	-219°	1.45	-180°
1	0.95	0.121	-201°	1.28	-175°
1^A	4.49	0.069	-279°	1.62	-218°
1^A	3.48	0.087	-266°	1.73	-208°
1^A	2.60	0.099	-246°	1.65	-196°
5	5.90	0.051	-301°	1.55	-240°
5	8.85	0.034	-340°	1.09	-263°
5	11.00	0.027	-350°	0.80	-268°
5	12.56	0.023	-355°	0.65	-270°
5	16.08	0.020	-358°	0.47	-
6	3.92	0.075	-	1.98	-
6	6.28	0.051	-313°	1.50	-250°
6	7.85	0.040	-321°	1.25	-260°
6	8.98	0.034	-345°	0.98	-265°
6	10.49	0.031	-	0.74	-
6	12.56	0.024	-	0.63	-
6	13.42	0.023	-	0.61	-
6	15.30	0.022	-	0.52	-
6	17.58	0.021	-	0.40	-

TABLE 4

Flight Condition

C.G. = 29.85% M.A.C.
V = 140 MPH
H_D = 5,000 Ft

Flight #	ω (rad/sec.)	$\frac{\lvert n_z \rvert}{\lvert \delta \rvert}$	$\phi_{n_{z\delta}}$	$\frac{\lvert \dot{\theta} \rvert}{\lvert \delta \rvert}$	$\phi_{\dot{\theta}\delta}$
2	4.20	0.191	-278°	2.95	-212°
2	3.78	0.211	-269°	2.94	-214°
2	3.34	0.233	-259°	2.94	-198°
2	3.41	0.223	-	2.96	-
2	2.66	0.253	-243°	3.00	-196°
2	2.04	0.274	-235°	2.71	-186°
2	1.41	0.298	-221°	2.58	-192°
3	4.94	0.179	-	2.97	-230°
3	4.19	0.207	-	2.90	-224°
3	2.96	0.252	-	3.22	-210°
3	2.14	0.300	-	2.81	-196°
3	1.70	0.302	-	2.79	-187°
4	5.03	0.184	-	2.87	-
4	4.22	0.202	-	3.01	-
4	3.38	0.234	-	2.93	-
4	2.40	0.268	-	2.83	-
4	1.49	0.304	-	2.54	-
5	16.70	0.0428	-	.965	-
5	13.45	0.0466	-	1.115	-
5	10.95	0.0695	-	1.545	-
5	8.68	0.0950	-	2.04	-
6	18.20	0.0395	-	0.685	-
6	12.20	0.0582	-355°	1.120	-270°
6	11.20	0.0654	-350°	1.290	-270°
6	10.80	0.0680	-350°	1.385	-270°
6	9.50	0.0800	-345°	1.620	-270°
6	8.30	0.0875	-330°	1.890	-268°
6	6.80	0.1150	-318°	2.400	-250°
6	4.98	0.1780	-280°	2.760	-224°

TABLE 5

Flight Condition

C.G. = 29.85% M.A.C.
V = 100 MPH
H_D = 5,000 Ft

Flight #	ω (rad/sec.)	$\frac{\lvert n_z \rvert}{\lvert \delta \rvert}$	$\phi_{n_z \delta}$	$\frac{\lvert \dot{\theta} \rvert}{\lvert \delta \rvert}$	$\phi_{\dot{\theta} \delta}$
2	4.79	0.0813	-	1.340	-
2	4.30	0.0908	-288°	1.772	-229°
2	3.30	0.1155	-260°	1.900	-206°
2	2.68	0.1335	-251°	1.900	-200°
2	2.09	0.1472	-233°	1.750	-192°
2	1.49	0.1680	-229°	0.814	-200°
3	4.64	0.0855	-	1.80	-
3	4.17	0.0861	-	1.84	-
3	3.06	0.1185	-	2.15	-
3	2.08	0.1295	-	2.04	-
3	1.75	0.1415	-	1.87	-191°
4	5.03	0.0624	-	1.75	-238°
4	4.23	0.0905	-	2.04	-222°
4	3.34	0.1070	-	2.23	-214°
4	2.34	0.1392	-	2.15	-196°
4	1.74	0.1610	-	1.91	-180°
5	18.10	0.0205	-	0.558	-
5	14.25	0.0212	-	0.600	-
5	11.90	0.0231	-	0.704	-
5	9.42	0.0271	-	0.880	-
5	6.72	0.0460	-	1.61	-
6	17.35	0.0233	-	0.467	-
6	15.20	0.0255	-	0.540	-
6	12.50	0.0275	-360°	0.623	-270°
6	12.20	0.0306	-350°	0.635	-270°
6	11.00	0.0306	-345°	0.719	-270°
6	9.86	0.0367	-340°	0.839	-262°
6	7.35	0.0428	-304°	1.100	-242°
6	6.15	0.0478	-305°	1.390	-237°
6	4.28	0.0815	-295°	1.870	-234°

TABLE 6

Flight Condition

C.G. = 34.6% M.A.C.
V = 140 MPH
H_D = 5,000 Ft

Flight #	ω (rad/sec.)	$\frac{\lvert n_z \rvert}{\lvert \delta \rvert}$	$\phi_{n_z \delta}$	$\frac{\lvert \dot{\theta} \rvert}{\lvert \delta \rvert}$	$\phi_{\dot{\theta} \delta}$
3	4.61	0.178	-293°	2.54	-242°
3	3.92	0.222	-283°	3.06	-230°
3	2.83	0.285	-263°	3.38	-216°
3	1.88	0.368	-245°	3.49	-205°
3	1.46	0.384	-220°	3.41	-190°
6	16.32	0.031	-	0.57	-
6	13.06	0.036	-	0.77	-
6	12.06	0.043	-	0.80	-
6	11.92	0.043	-	0.83	-
6	11.00	0.046	-	1.02	-
6	8.61	0.063	-326°	1.29	-264°
6	7.16	0.077	-322°	1.49	-257°
6	5.71	0.107	-305°	1.88	-250°

TABLE 7

Flight Condition

C.G. = 34.6% M.A.C.
V = 100 MPH
H_D = 5,000 Ft

Flight #	ω (rad/sec.)	$\frac{\lvert n_z \rvert}{\lvert \delta \rvert}$	$\phi_{n_{z}\delta}$	$\frac{\lvert \dot{\theta} \rvert}{\lvert \delta \rvert}$	$\phi_{\dot{\theta}\delta}$
3	4.61	0.074	-308°	1.66	-234°
3	4.18	0.083	-292°	1.86	-228°
3	3.26	0.099	-284°	2.02	-216°
3	2.42	0.132	-272°	2.32	-212°
3	1.58	0.193	-246°	2.51	-206°
6	4.71	0.068	-310°	1.50	-238°
6	6.28	0.035	-323°	0.98	-244°
6	7.85	0.027	-350°	0.75	-250°
6	10.10	0.023	-355°	0.59	-268°
6	10.80	0.022	-357°	0.54	-270°
6	12.07	0.021	-360°	0.50	-270°
6	13.20	0.020	-	0.43	-
6	15.08	0.018	-	0.40	-
6	18.83	0.013	-	0.25	-

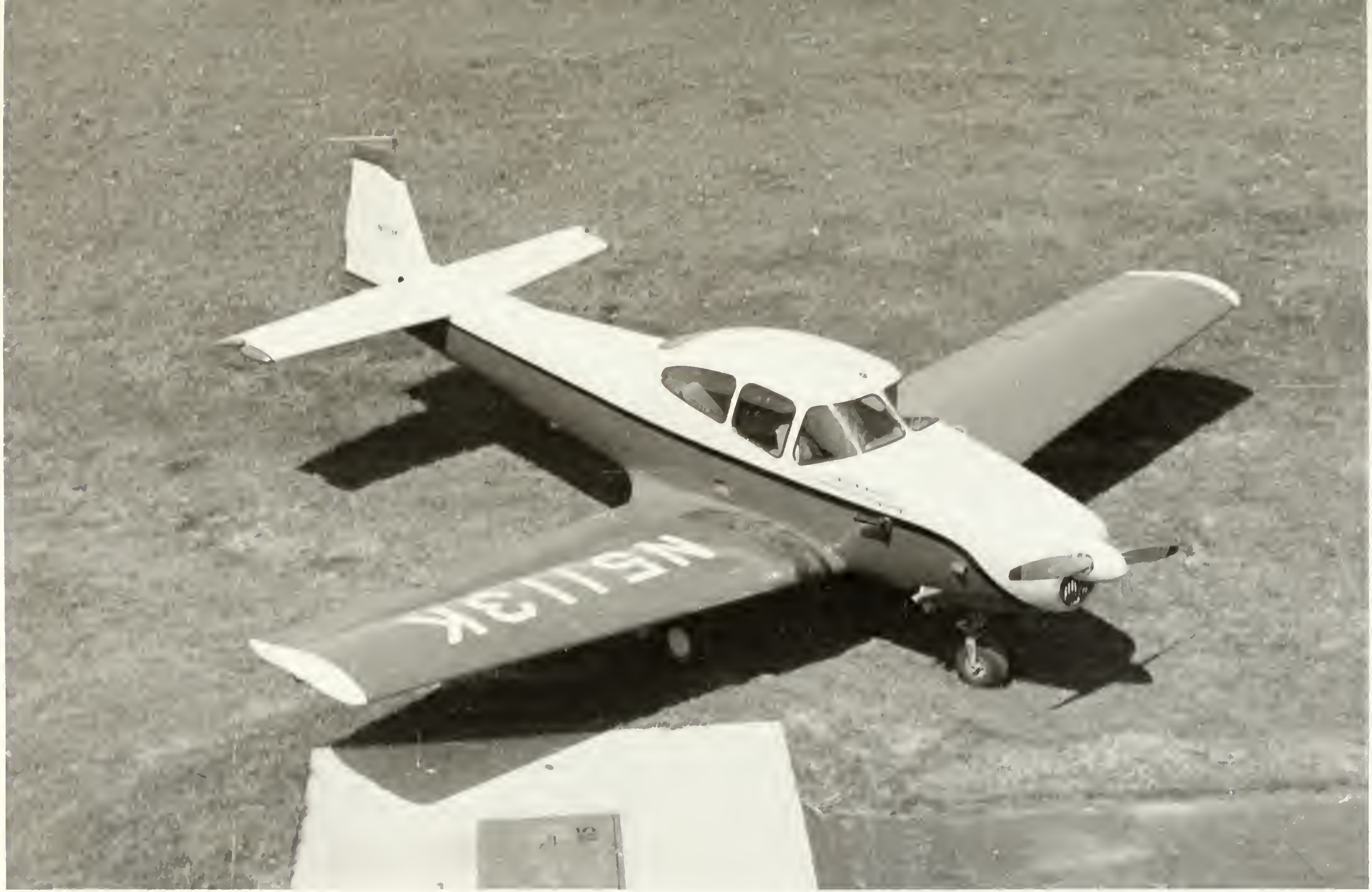

TEST AIRPLANE
FIG. 1

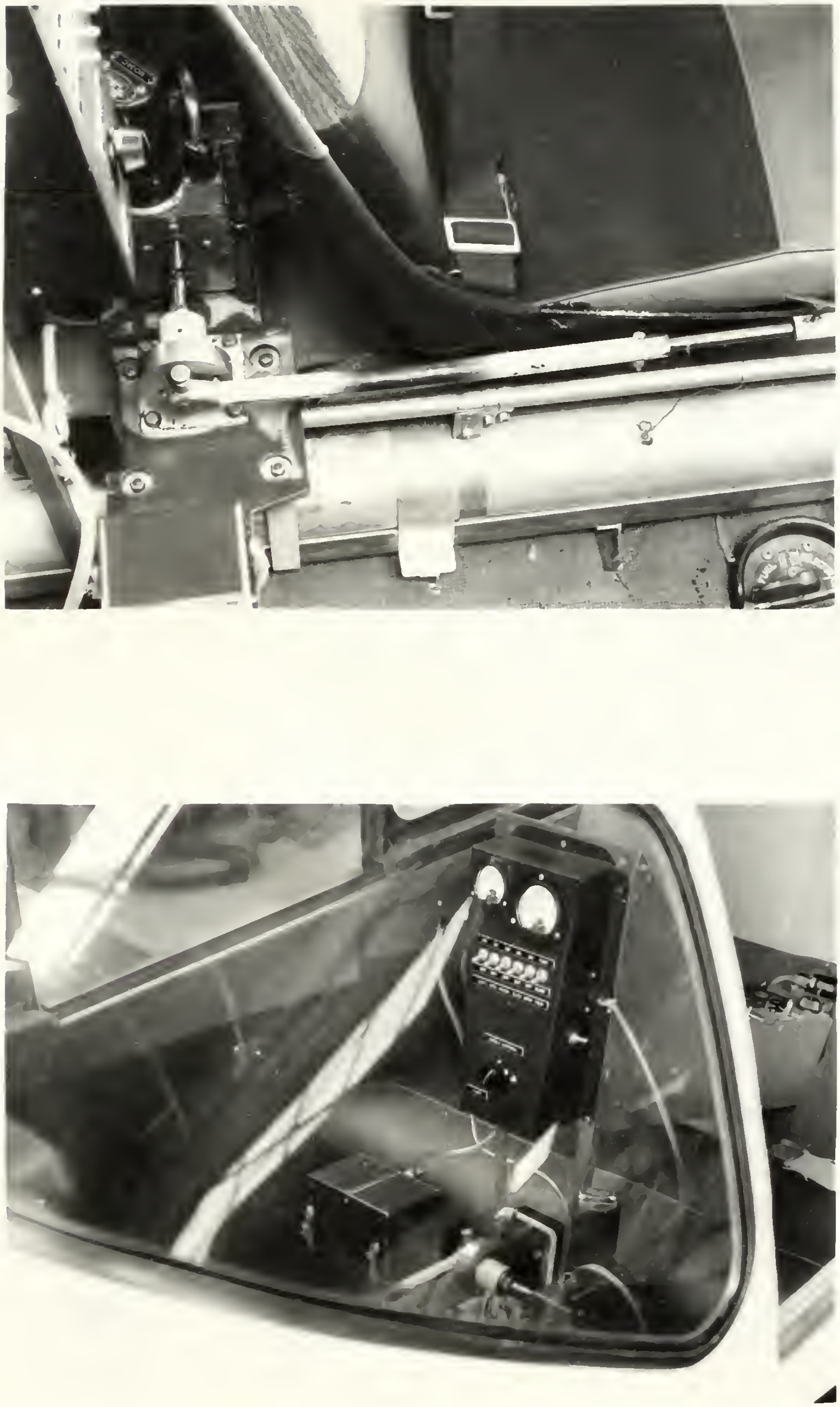

CONTROL PANEL AND ASSEMBLED
INSTRUMENTATION COMPONENTS
FIG.2

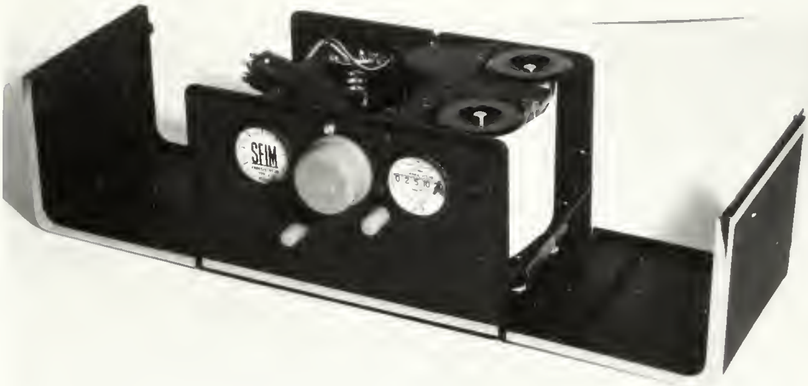

FIG. 3 SFIM RECORDER

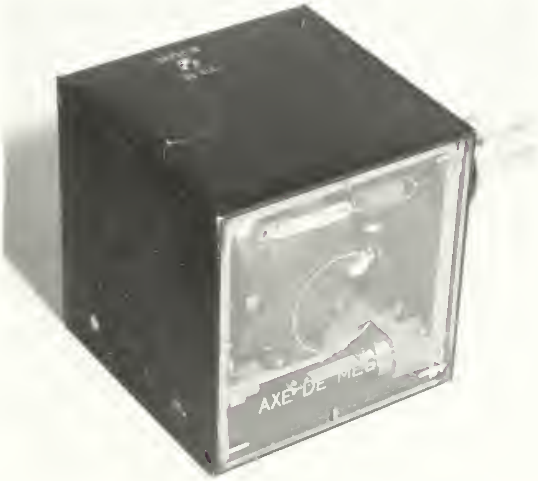

FIG. 4 RATE OF TURN GYRO TRANSMITTER

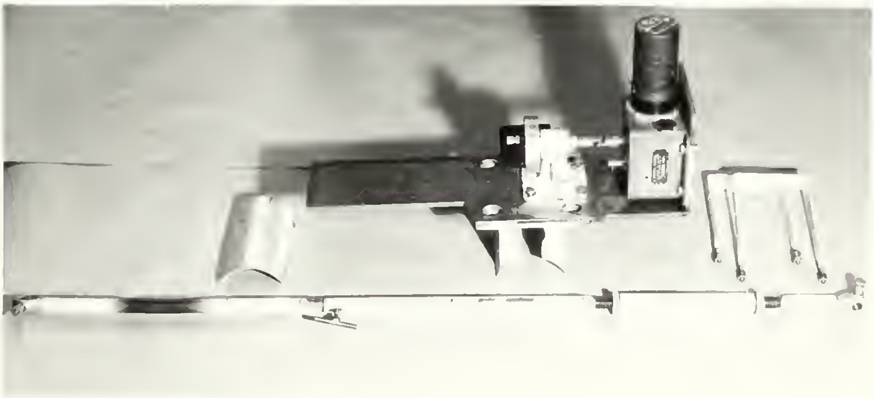

ELEVATOR OSCILLATING MOTOR, WHEEL, SUPPORT, AND DRIVE SHAFT

FIG. 5

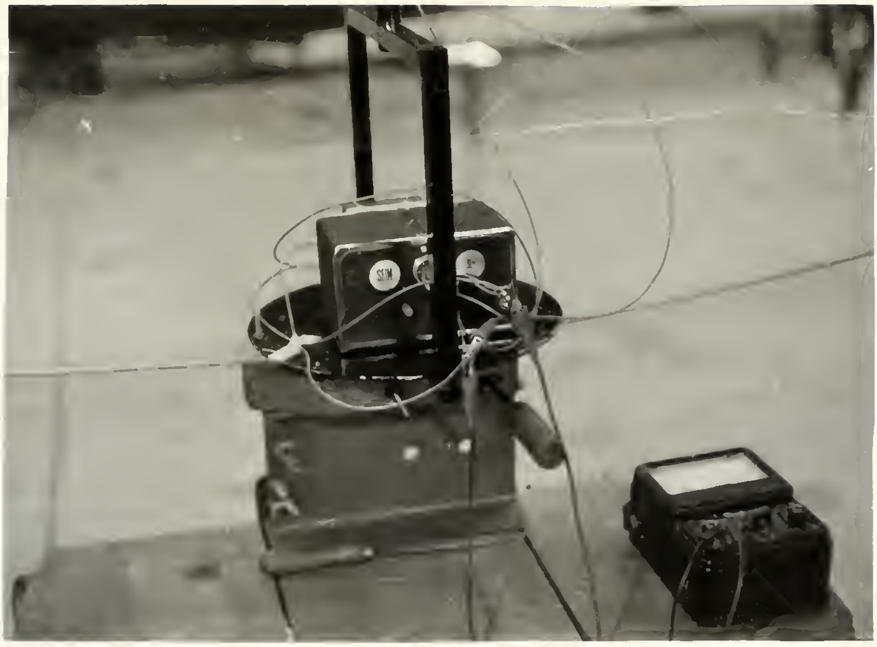

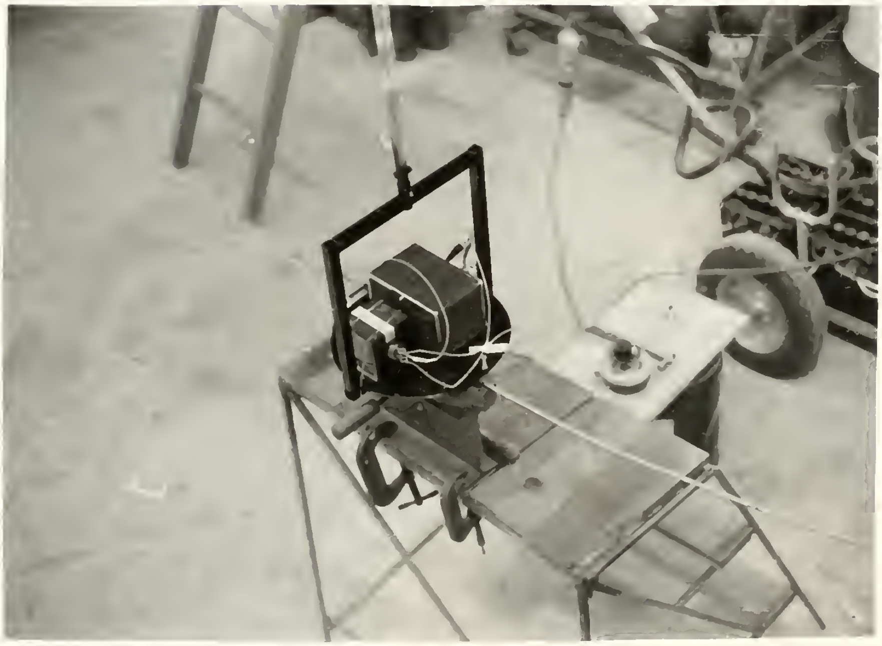

RATE OF TURN GYRO TRANSMITTER
CALIBRATION EQUIPMENT
FIG. 6

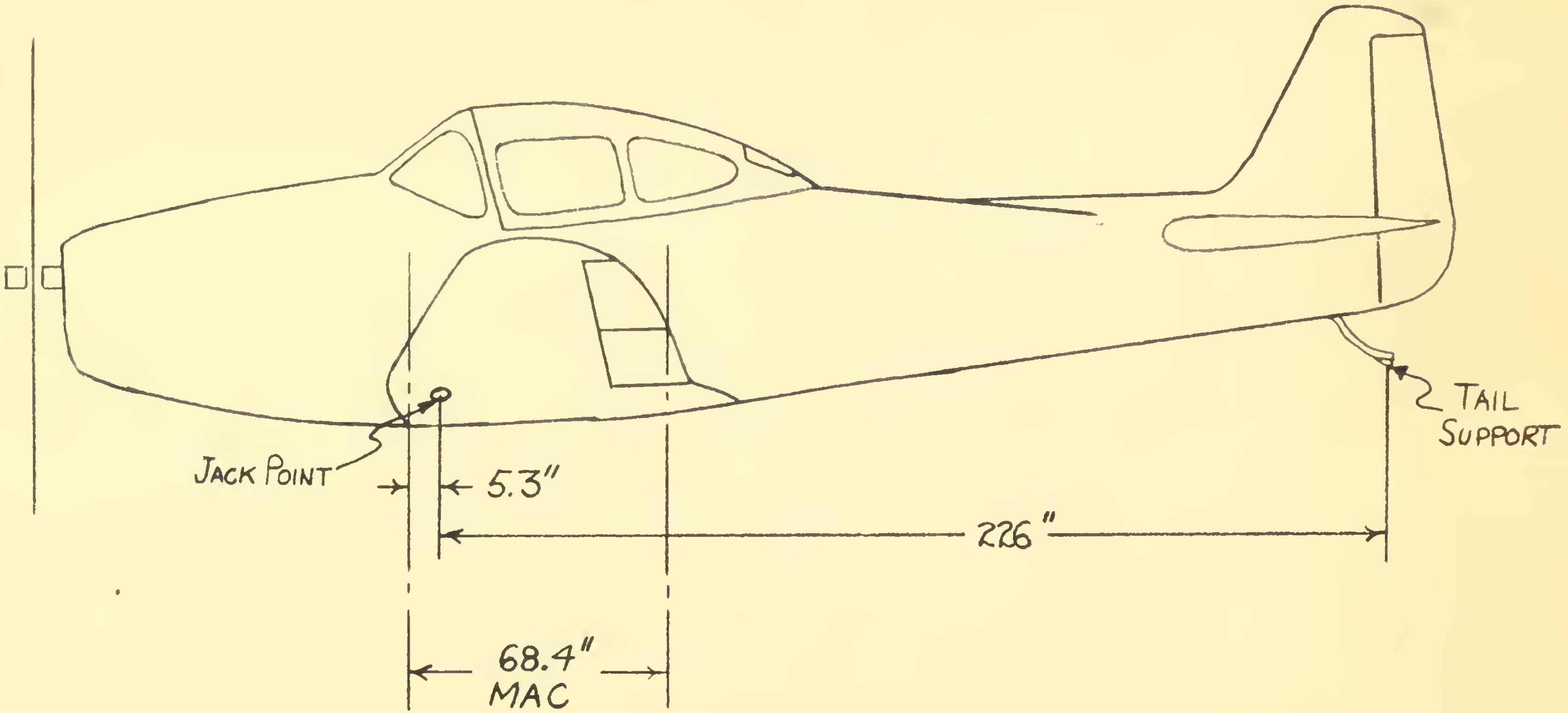
TAIL SUPPORT
JACK POINT
5.3"
226"
68.4"
MAC

AIRPLANE C.G. DETERMINATION MEASUREMENTS

FIG. 7

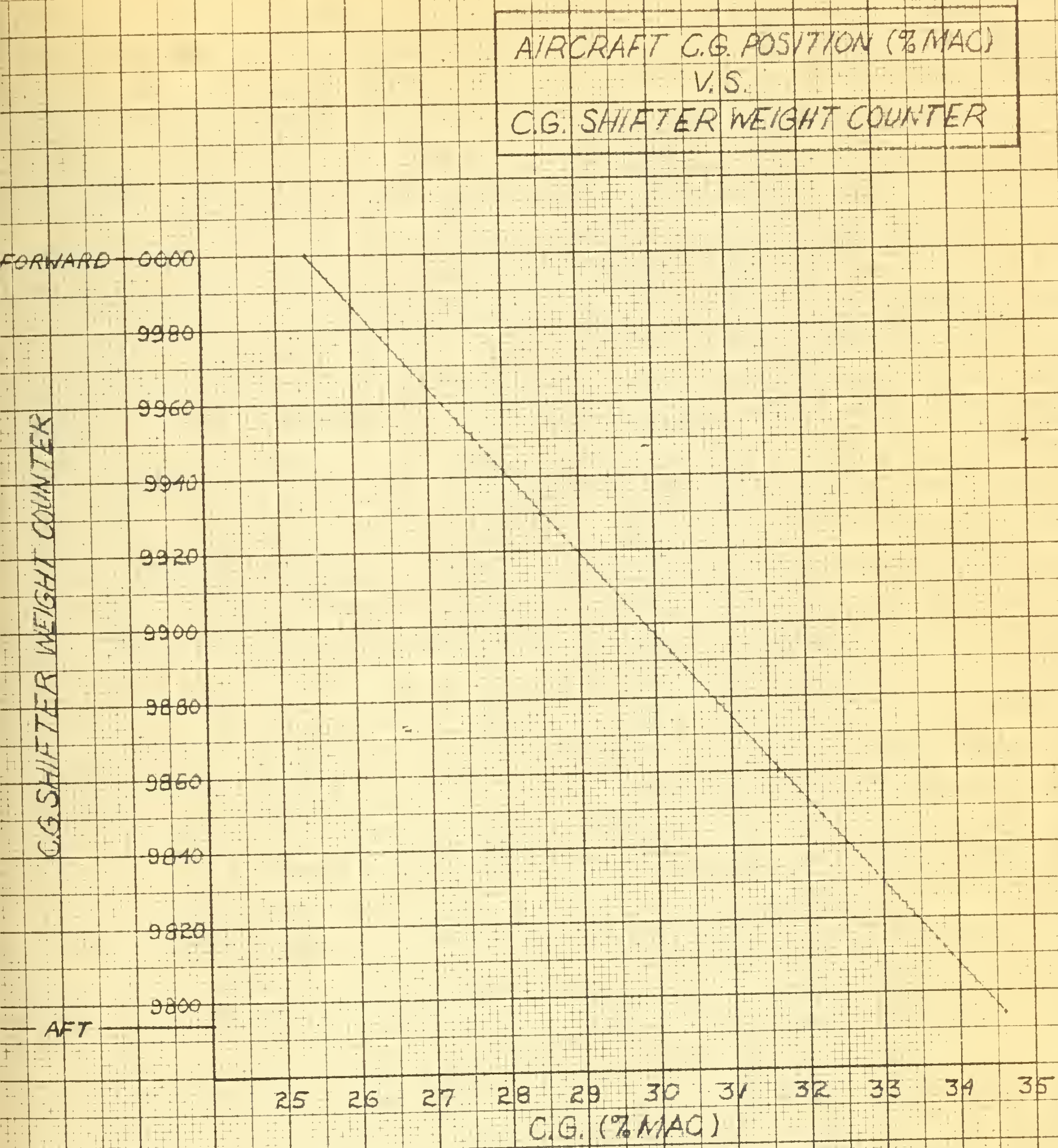
AIRCRAFT C.G. POSITION (% MAC)
V.S.
C.G. SHIFTER WEIGHT COUNTER
C.G. SHIFTER WEIGHT COUNTER
FORWARD
0000
9980
9960
9940
9920
9900
9880
9860
9840
9820
9800
AFT
25
26
27
28
29
30
31
32
33
34
35
C.G. (% MAC)

FIG. 8

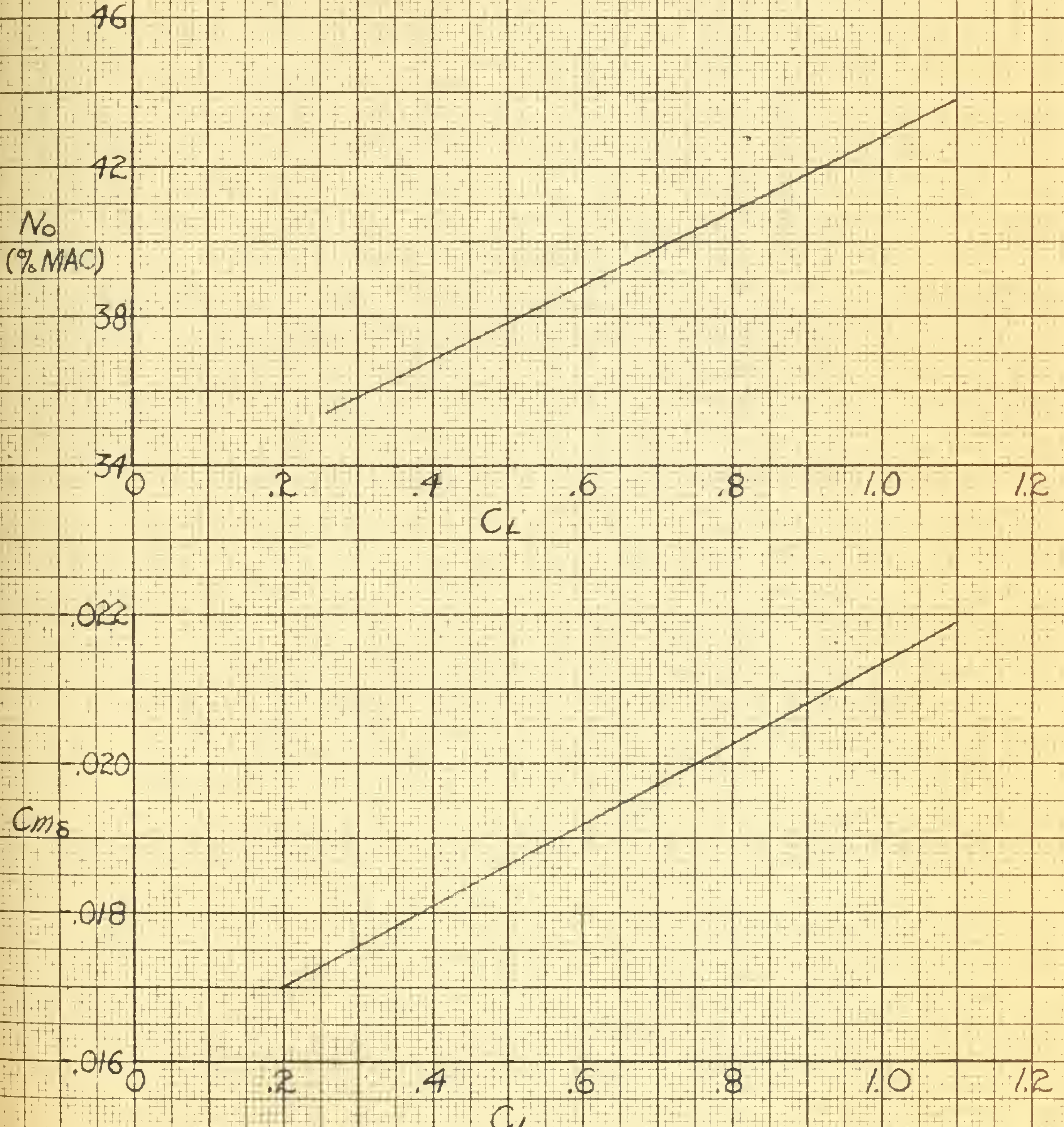

VARIATION OF STICK FIXED NEUTRAL POINT (N_0) AND ELEVATOR POWER (C_{m_δ}) v.s. LIFT COEFFICIENT

NAVION N-5113K - POWER ON, GEAR & FLAPS UP

(FROM PRINCETON AERONAUTICAL ENGINEERING REPORT #225)

FIG. 9

SAMPLES OF GOOD SFIM RECORDER FILM DATA

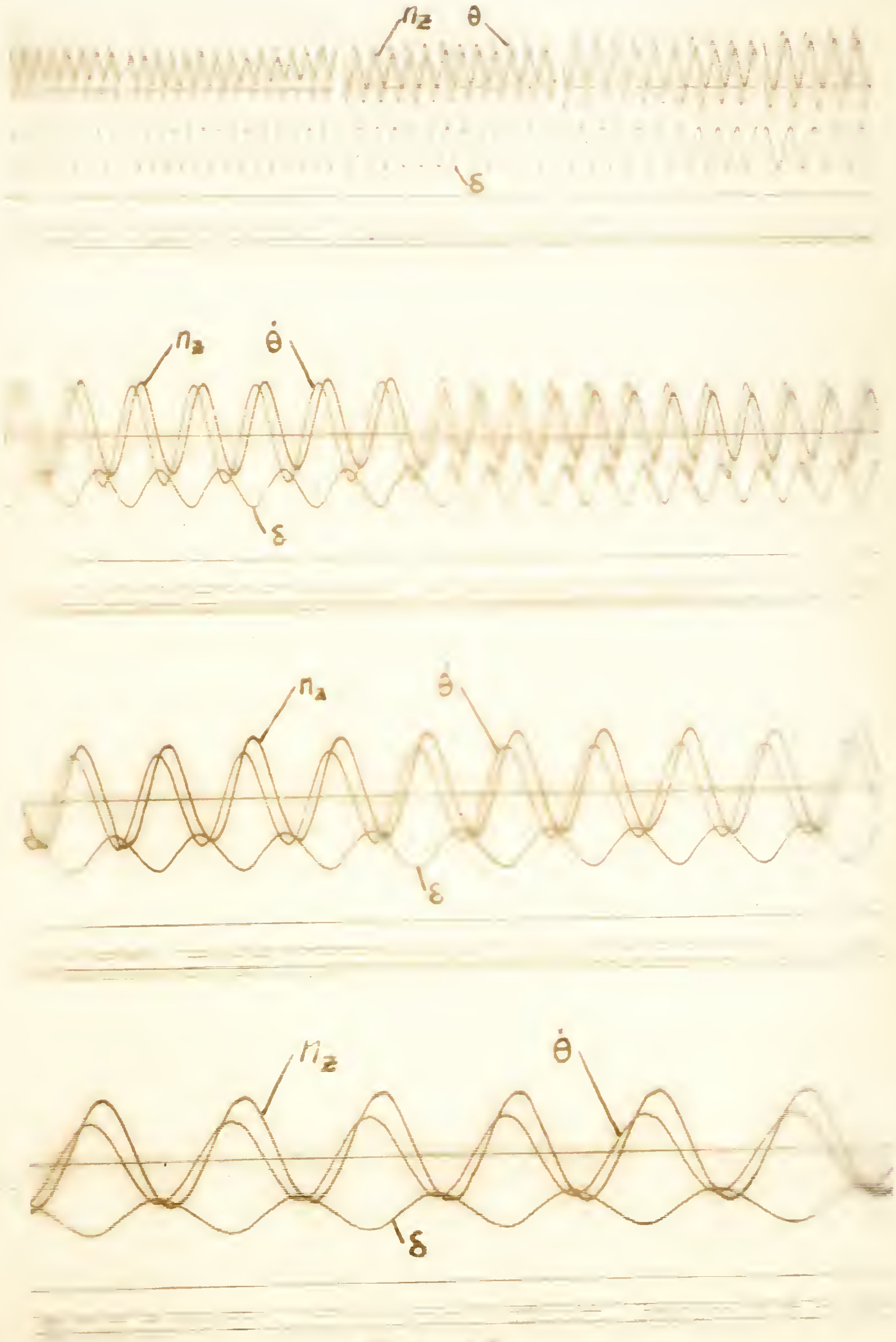

FIG. 10

SAMPLES OF POOR SFIM RECORDER FILM DATA

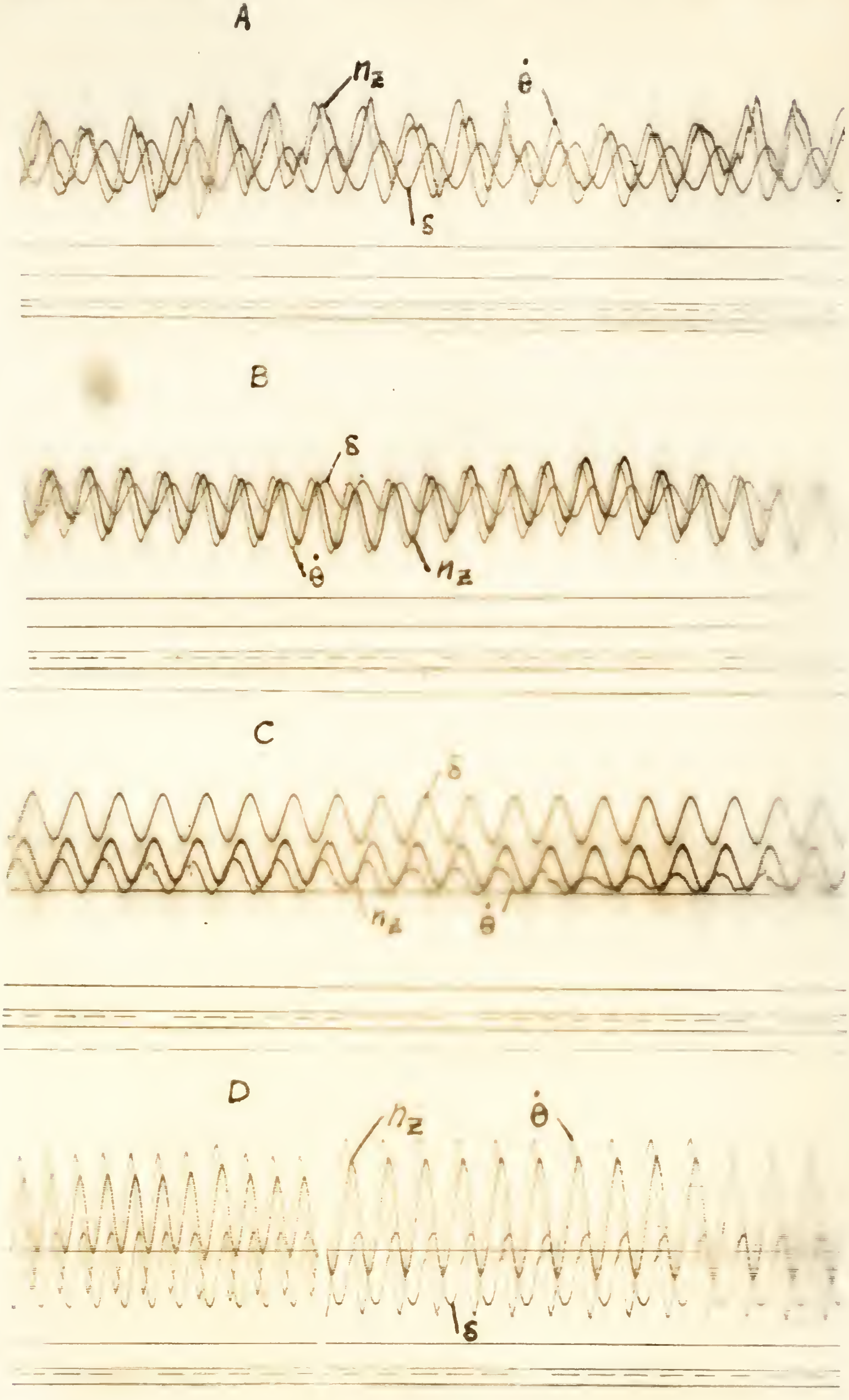

FIG 11

NORMAL ACCELERATION FREQUENCY RESPONSE

AMPLITUDE RATIO AND PHASE ANGLE VS.
FREQUENCY OF ELEVATOR OSCILLATION

FLIGHT CONDITION: C.G. = 25.4 % M.A.C.
H_D = 5000 FEET   V = 140 M.P.H.

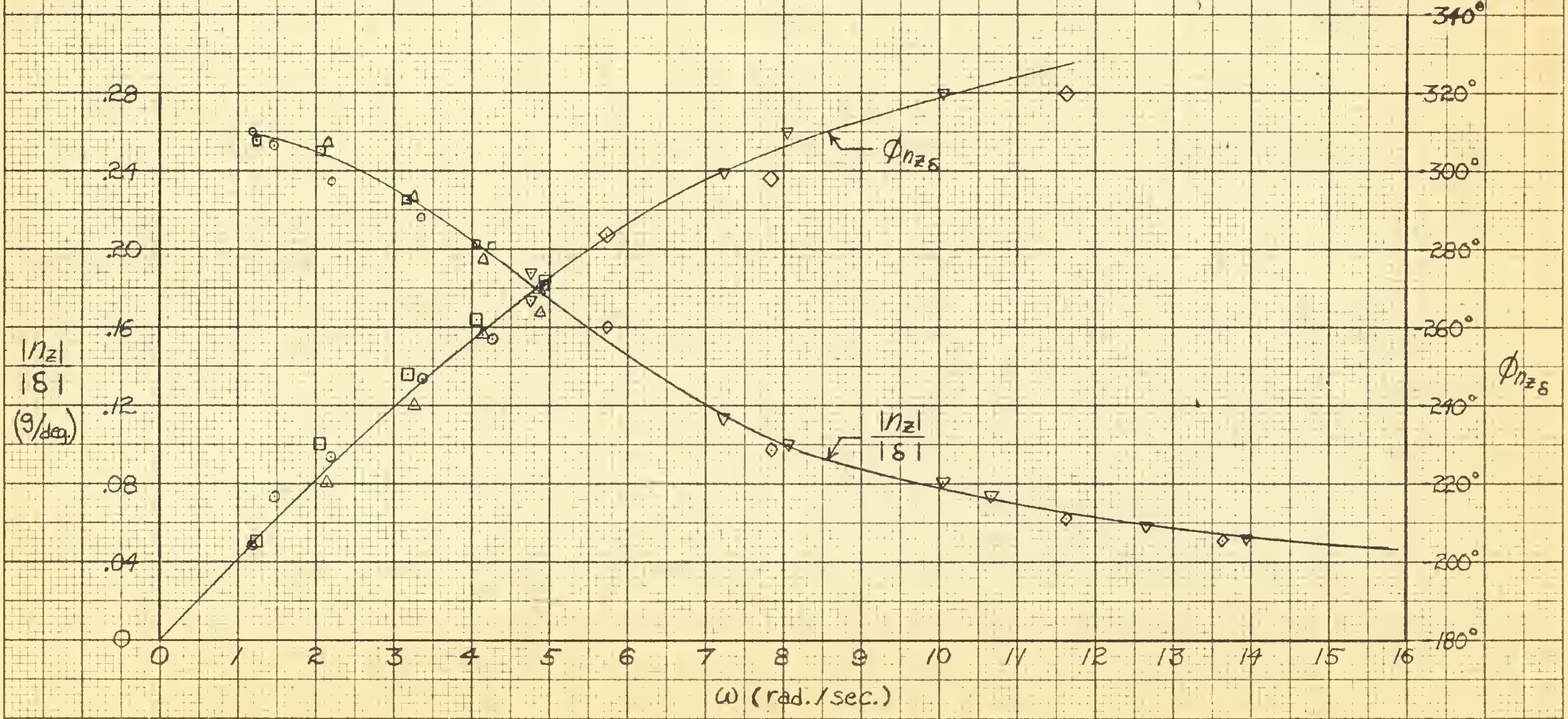

FIG. 12

PITCH RATE FREQUENCY RESPONSE

AMPLITUDE RATIO AND PHASE ANGLE VS. FREQUENCY OF ELEVATOR OSCILLATION

FLIGHT CONDITION : C.G. = 25.4% MAC
H_D = 5000 FEET V = 140 M.P.H.

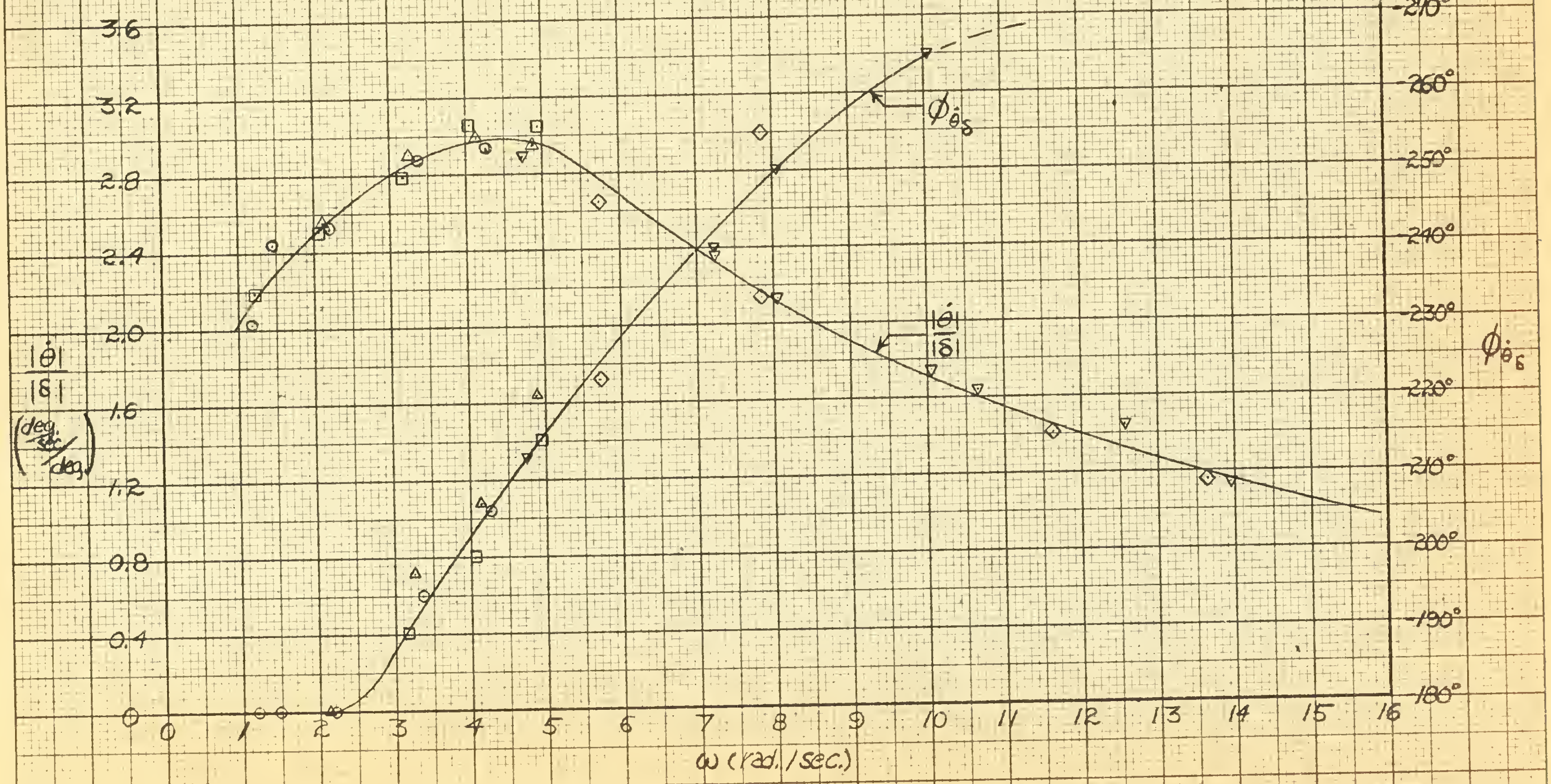

FIG. 13

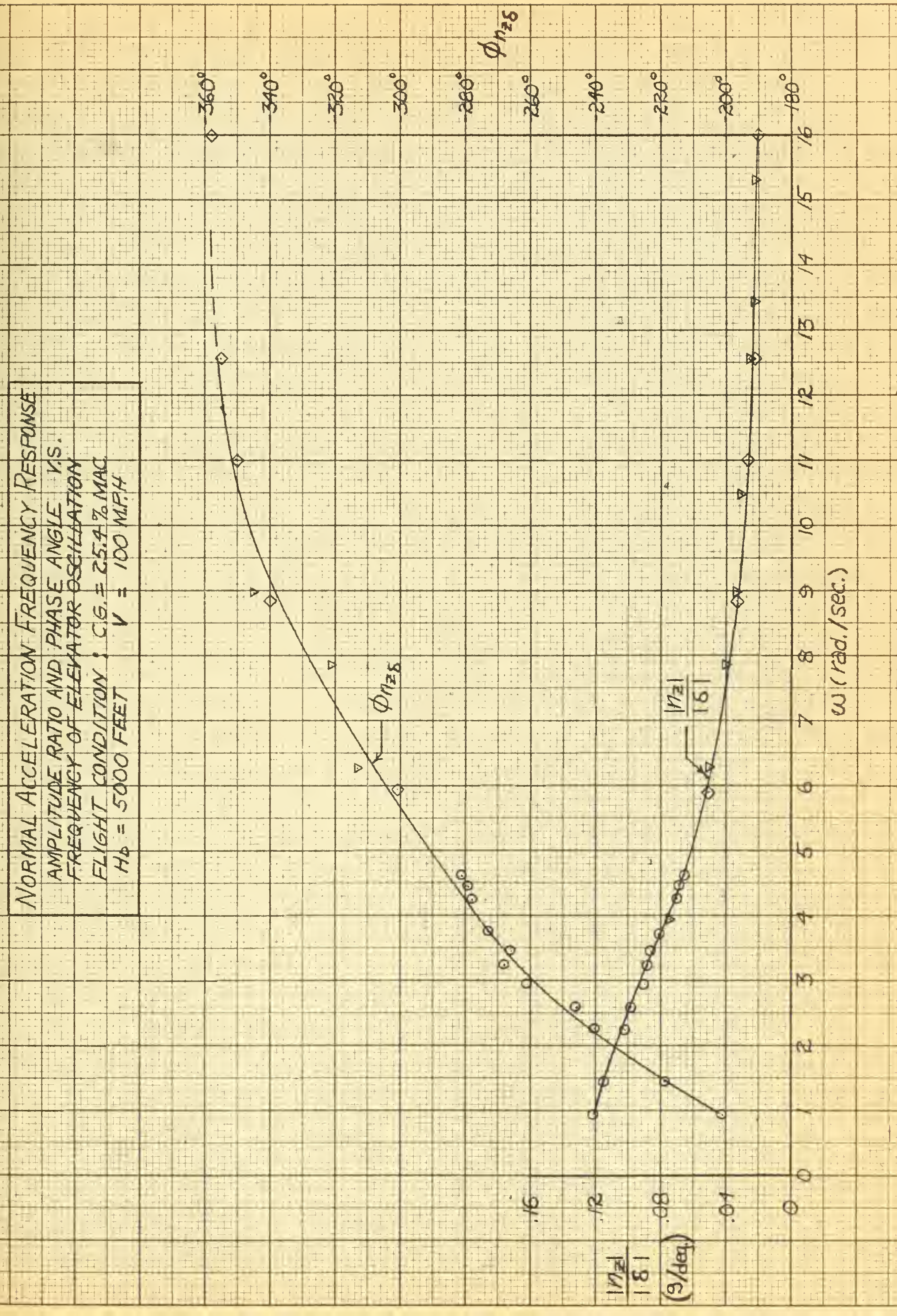
NORMAL ACCELERATION FREQUENCY RESPONSE
AMPLITUDE RATIO AND PHASE ANGLE V.S.
FREQUENCY OF ELEVATOR OSCILLATION
FLIGHT CONDITION : C.G. = 25.4 % MAC
Hp = 5000 FEET   V = 100 M.P.H
$\phi_{n_z\delta}$
$\frac{|n_z|}{|\delta|}$
$\frac{|n_z|}{|\delta|}$ (g/deg.)
0
.04
.08
.12
.16
360°
340°
320°
300°
280°
260°
240°
220°
200°
180°
0
1
2
3
4
5
6
7
8
9
10
11
12
13
14
15
16
ω (rad./sec.)

FIG. 14

PITCH RATE FREQUENCY RESPONSE

AMPLITUDE RATIO AND PHASE ANGLE V.S. ~~FREQUENCY OF ELEVATOR OSCILLATION~~

FLIGHT CONDITION : C.G. = 25.4 % M.A.C.
H_D = 5000 FEET V = 100 M.P.H.

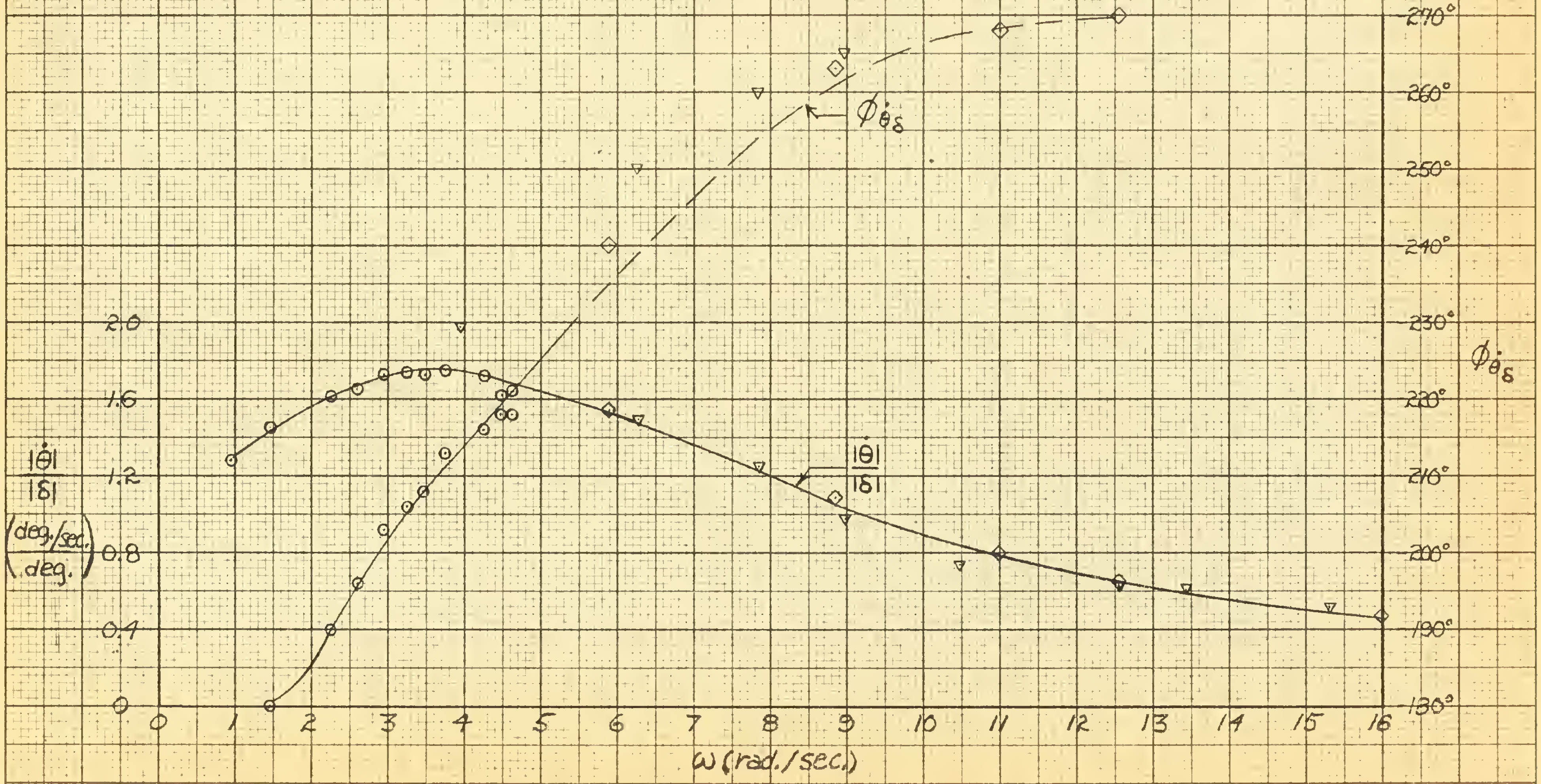

FIG. 15

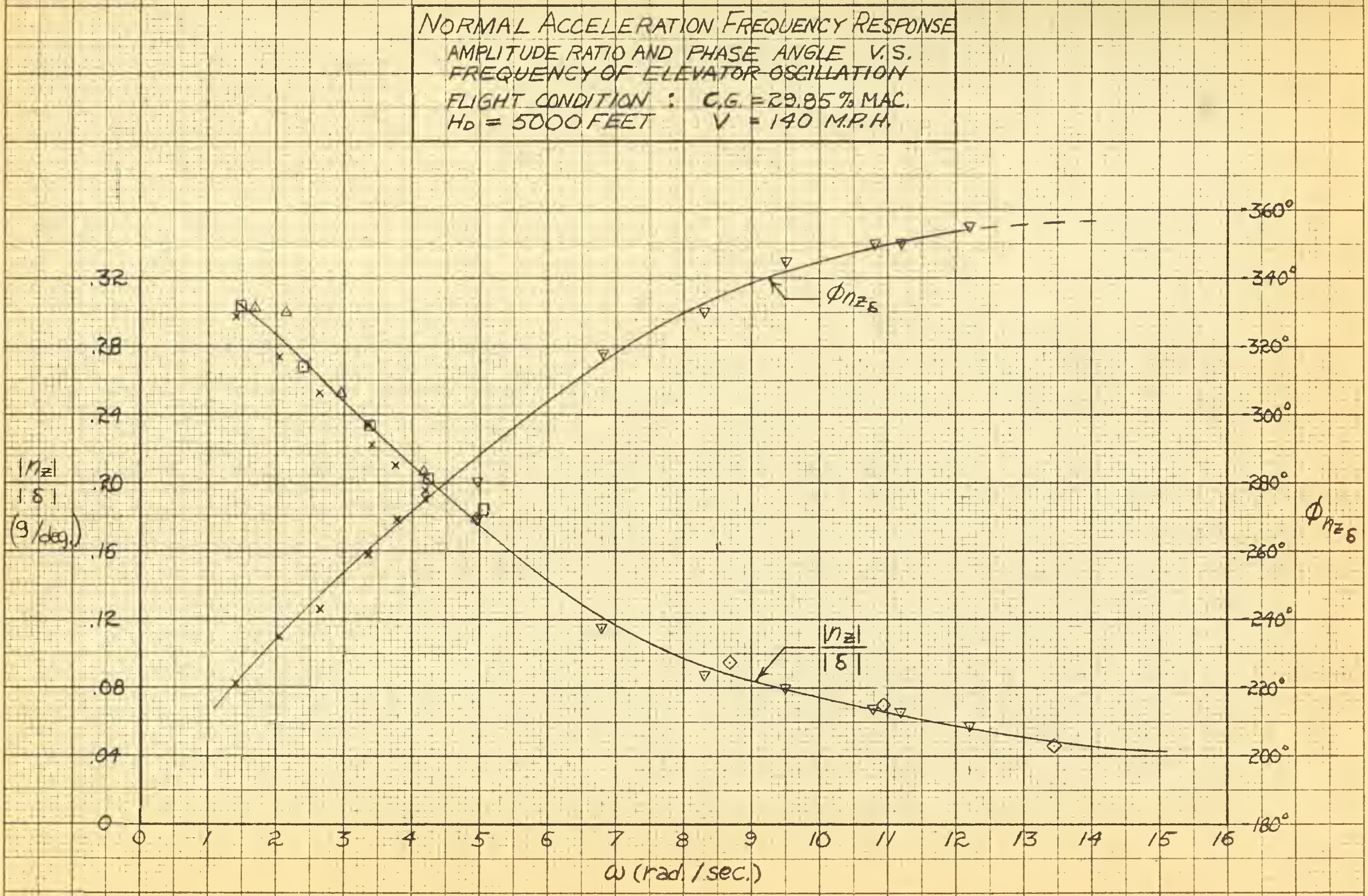

NORMAL ACCELERATION FREQUENCY RESPONSE
AMPLITUDE RATIO AND PHASE ANGLE V.S.
~~FREQUENCY OF ELEVATOR OSCILLATION~~
FLIGHT CONDITION : C.G. = 29.85 % MAC.
H_D = 5000 FEET V = 140 M.P.H.

FIG. 16

PITCH RATE FREQUENCY RESPONSE

AMPLITUDE RATIO AND PHASE ANGLE V.S.
FREQUENCY OF ELEVATOR OSCILLATION

FLIGHT CONDITION: C.G. = 29.85% M.A.C.
H_D = 5000 FEET V = 140 M.P.H.

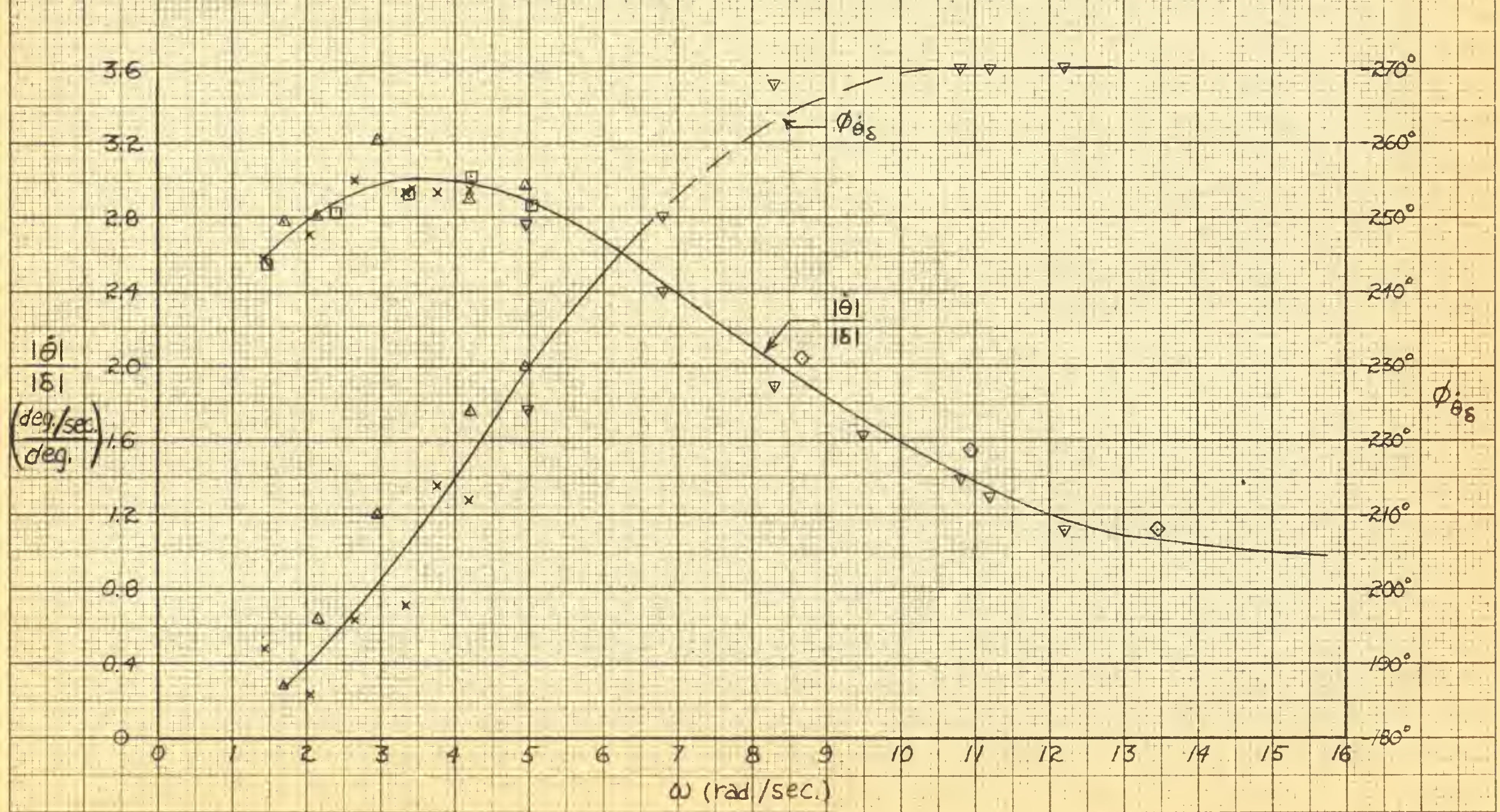

FIG. 17

NORMAL ACCELERATION FREQUENCY RESPONSE
AMPLITUDE RATIO AND PHASE ANGLE V.S.
FREQUENCY OF ELEVATOR OSCILLATION
FLIGHT CONDITION: C.G. = 29.85% M.A.C.
H_D = 5000 FEET V = 100 M.P.H.

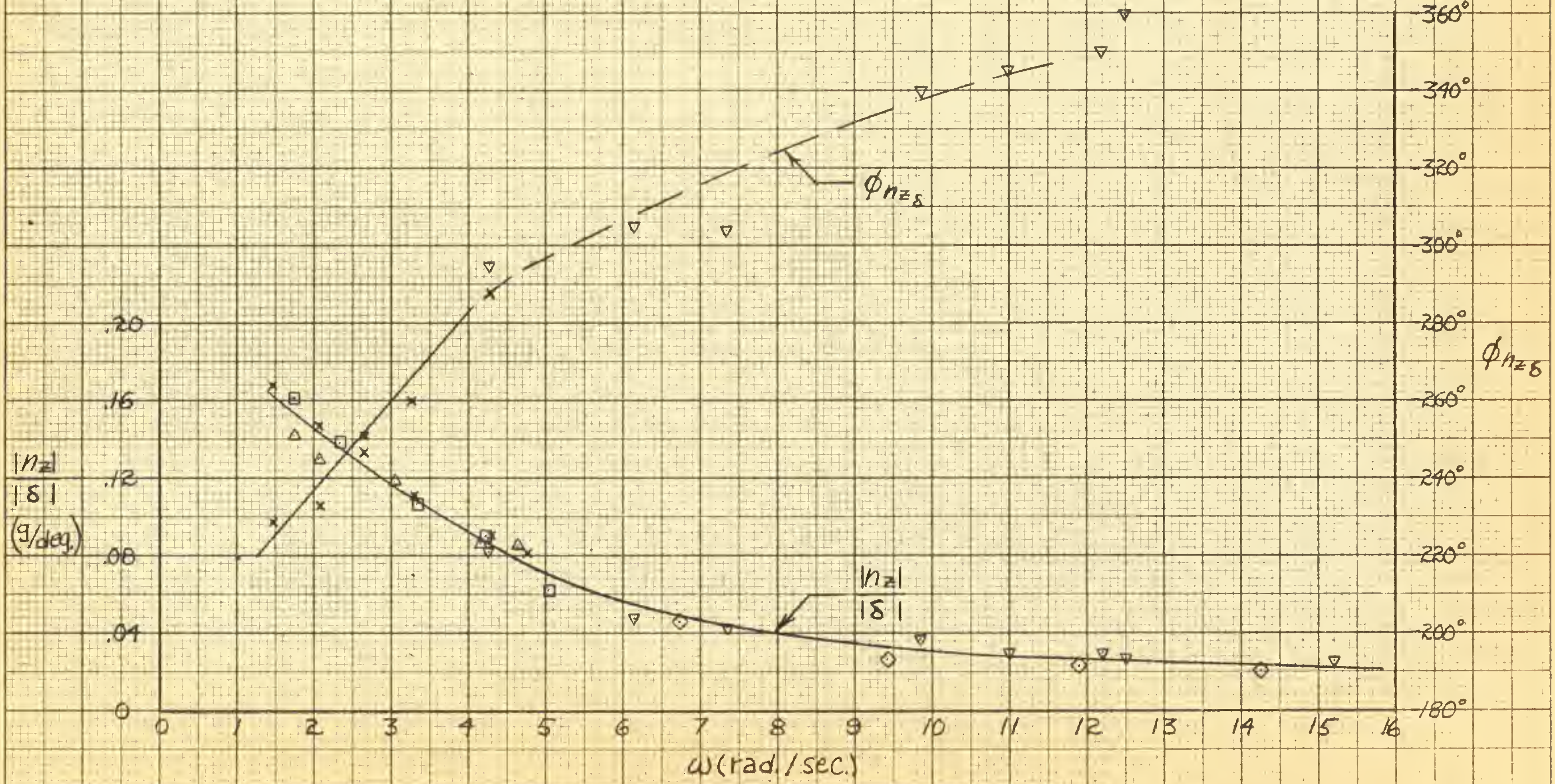

FIG. 18

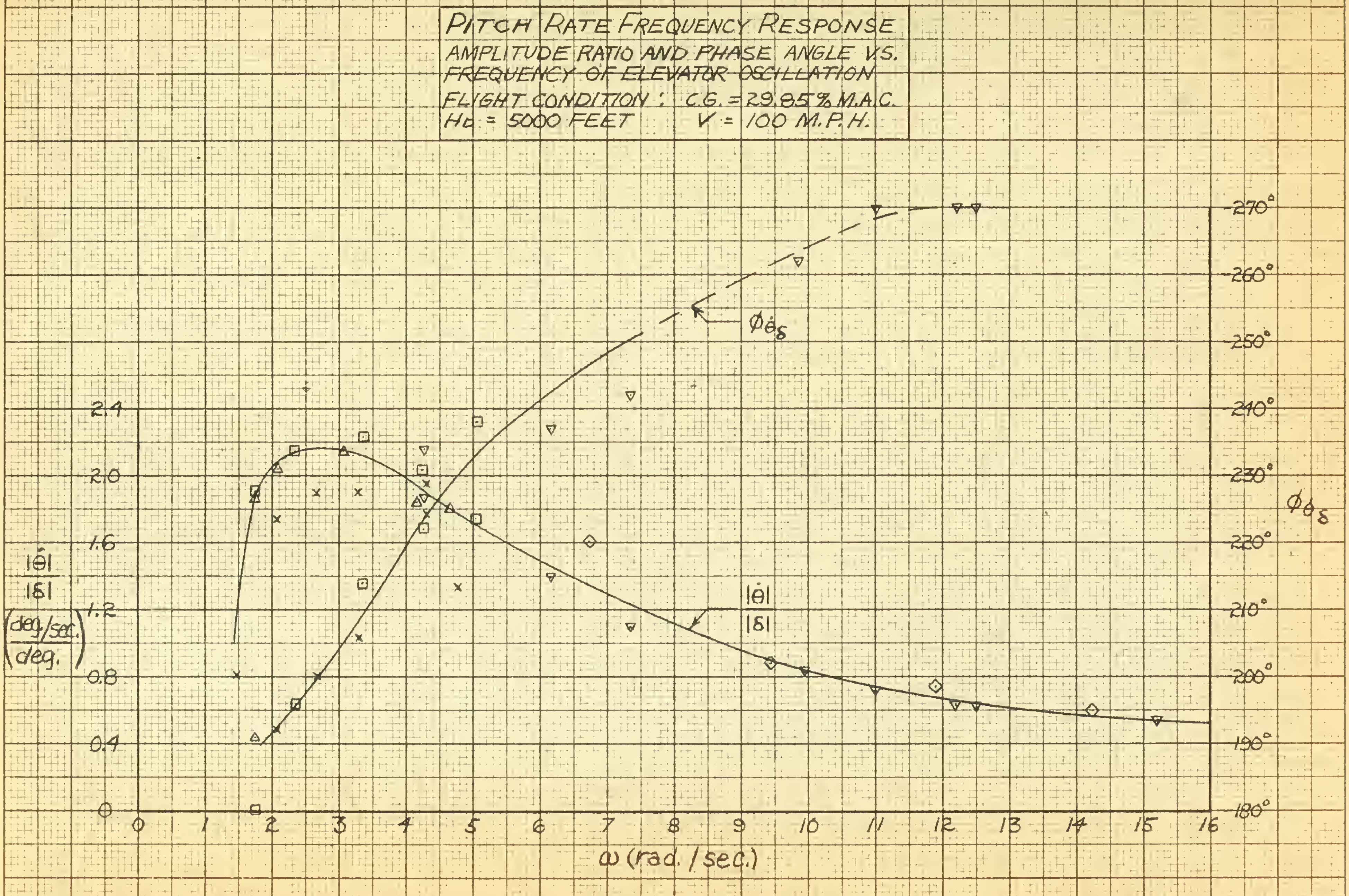
PITCH RATE FREQUENCY RESPONSE
AMPLITUDE RATIO AND PHASE ANGLE VS.
FREQUENCY OF ELEVATOR OSCILLATION
FLIGHT CONDITION : C.G. = 29.85% M.A.C.
Hb = 5000 FEET V = 100 M.P.H.
$\frac{|\dot{\theta}|}{|\delta|}$ $\left(\frac{deg./sec.}{deg.}\right)$
0
0.4
0.8
1.2
1.6
2.0
2.4
$\phi_{\dot{\theta}\delta}$
180°
190°
200°
210°
220°
230°
240°
250°
260°
270°
$\phi_{\dot{\theta}\delta}$
$\frac{|\dot{\theta}|}{|\delta|}$
0
1
2
3
4
5
6
7
8
9
10
11
12
13
14
15
16
ω (rad. / sec.)

FIG. 19

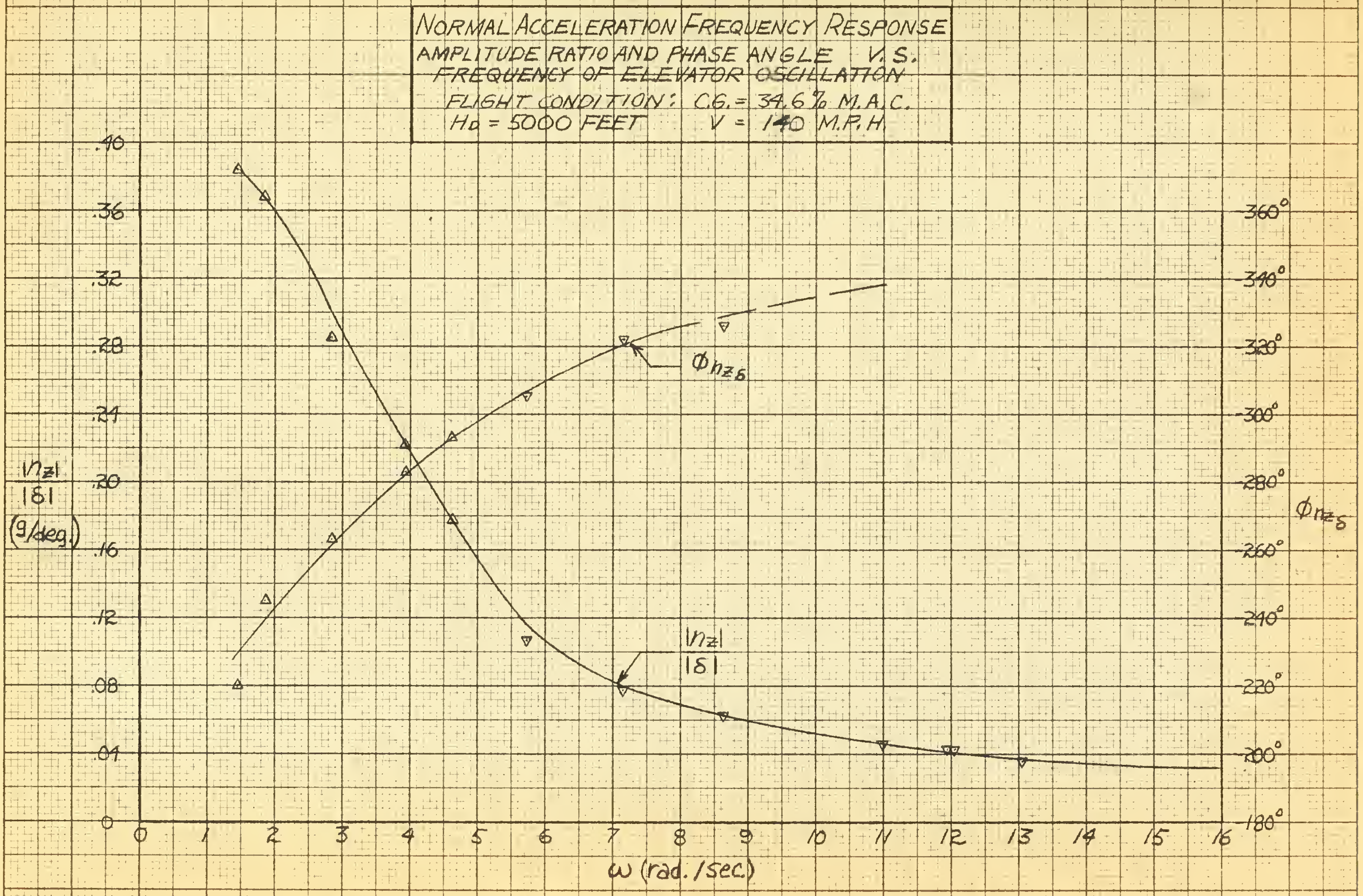
NORMAL ACCELERATION FREQUENCY RESPONSE
AMPLITUDE RATIO AND PHASE ANGLE V.S.
FREQUENCY OF ELEVATOR OSCILLATION
FLIGHT CONDITION: C.G. = 34.6 % M.A.C.
H_D = 5000 FEET V = 140 M.P.H.

FIG. 20

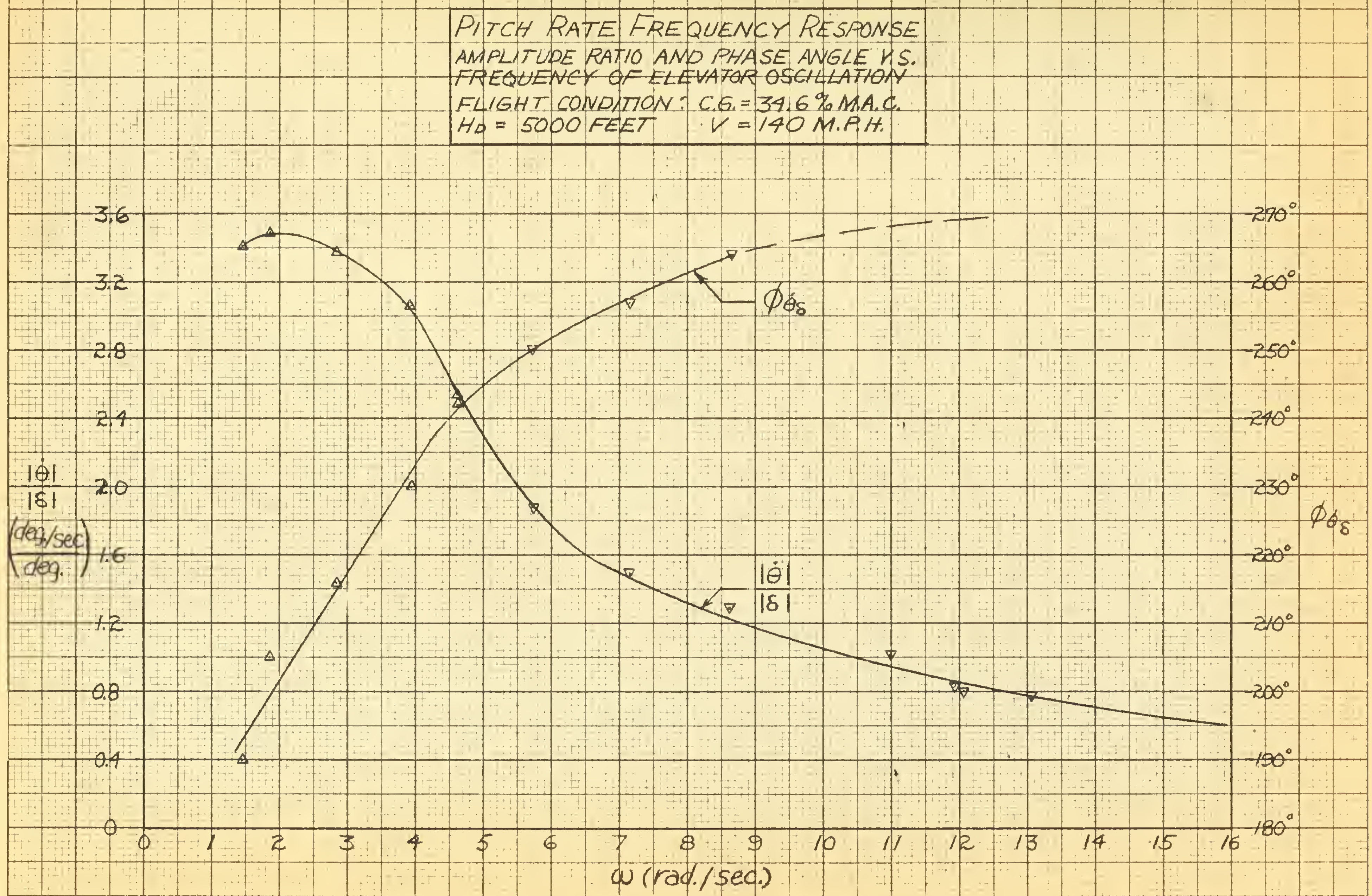
PITCH RATE FREQUENCY RESPONSE
AMPLITUDE RATIO AND PHASE ANGLE V.S. FREQUENCY OF ELEVATOR OSCILLATION
FLIGHT CONDITION: C.G. = 34.6% M.A.C.
H_D = 5000 FEET V = 140 M.P.H.
$\frac{|\dot{\theta}|}{|\delta|}$ $\left(\frac{deg./sec}{deg.}\right)$
3.6
3.2
2.8
2.4
2.0
1.6
1.2
0.8
0.4
0
$\phi_{\dot{\theta}_\delta}$
270°
260°
250°
240°
230°
220°
210°
200°
190°
180°
$\phi_{\dot{\theta}_\delta}$
$\frac{|\dot{\theta}|}{|\delta|}$
0
1
2
3
4
5
6
7
8
9
10
11
12
13
14
15
16
ω (rad./sec.)

FIG. 21

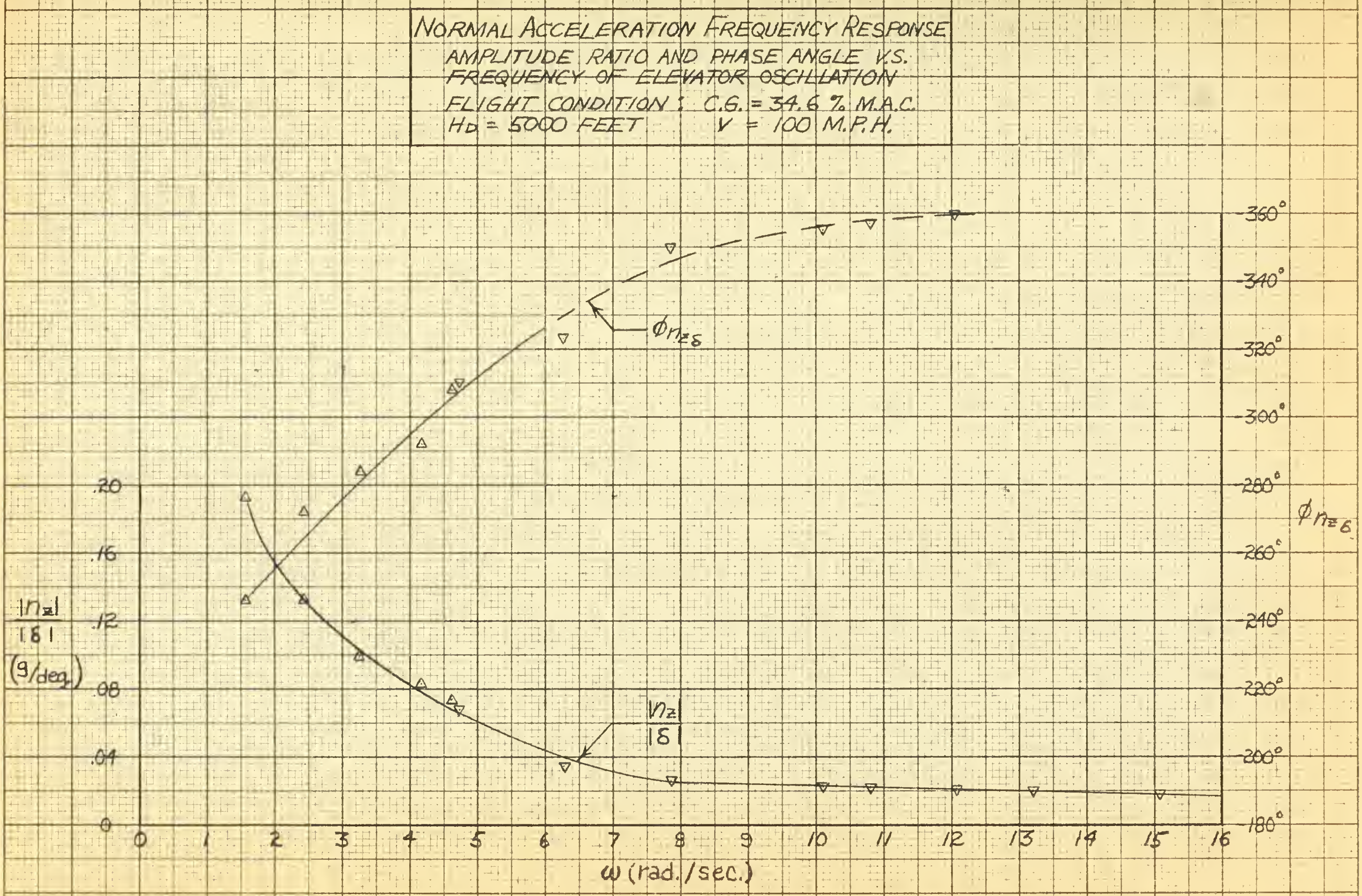

NORMAL ACCELERATION FREQUENCY RESPONSE
AMPLITUDE RATIO AND PHASE ANGLE V.S. FREQUENCY OF ELEVATOR OSCILLATION
FLIGHT CONDITION: C.G. = 34.6 % M.A.C.
H_D = 5000 FEET V = 100 M.P.H.

FIG. 22

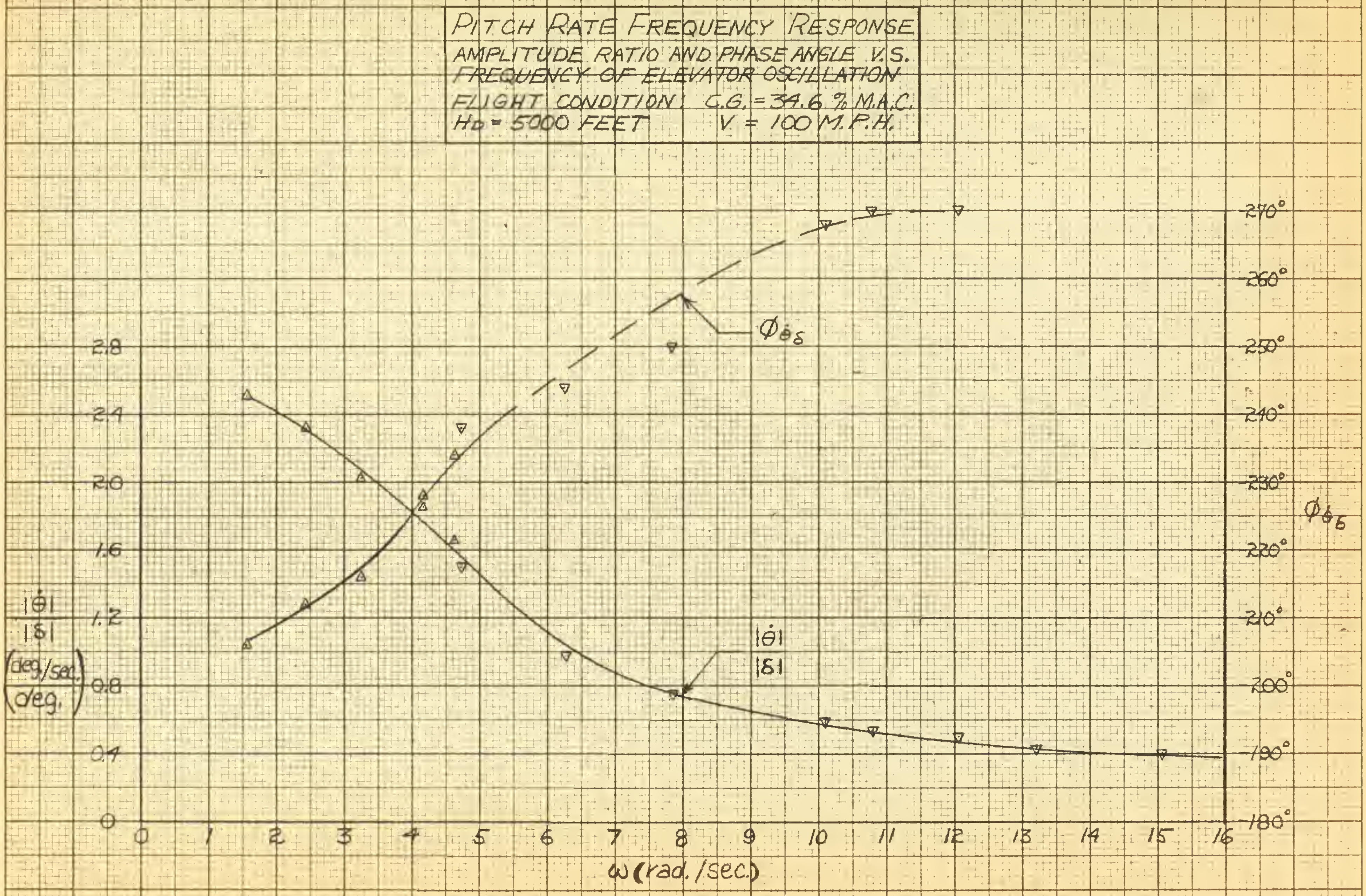

PITCH RATE FREQUENCY RESPONSE
AMPLITUDE RATIO AND PHASE ANGLE V.S. FREQUENCY OF ELEVATOR OSCILLATION
FLIGHT CONDITION: C.G. = 34.6 % M.A.C.
H_D = 5000 FEET V = 100 M.P.H.

FIG. 23

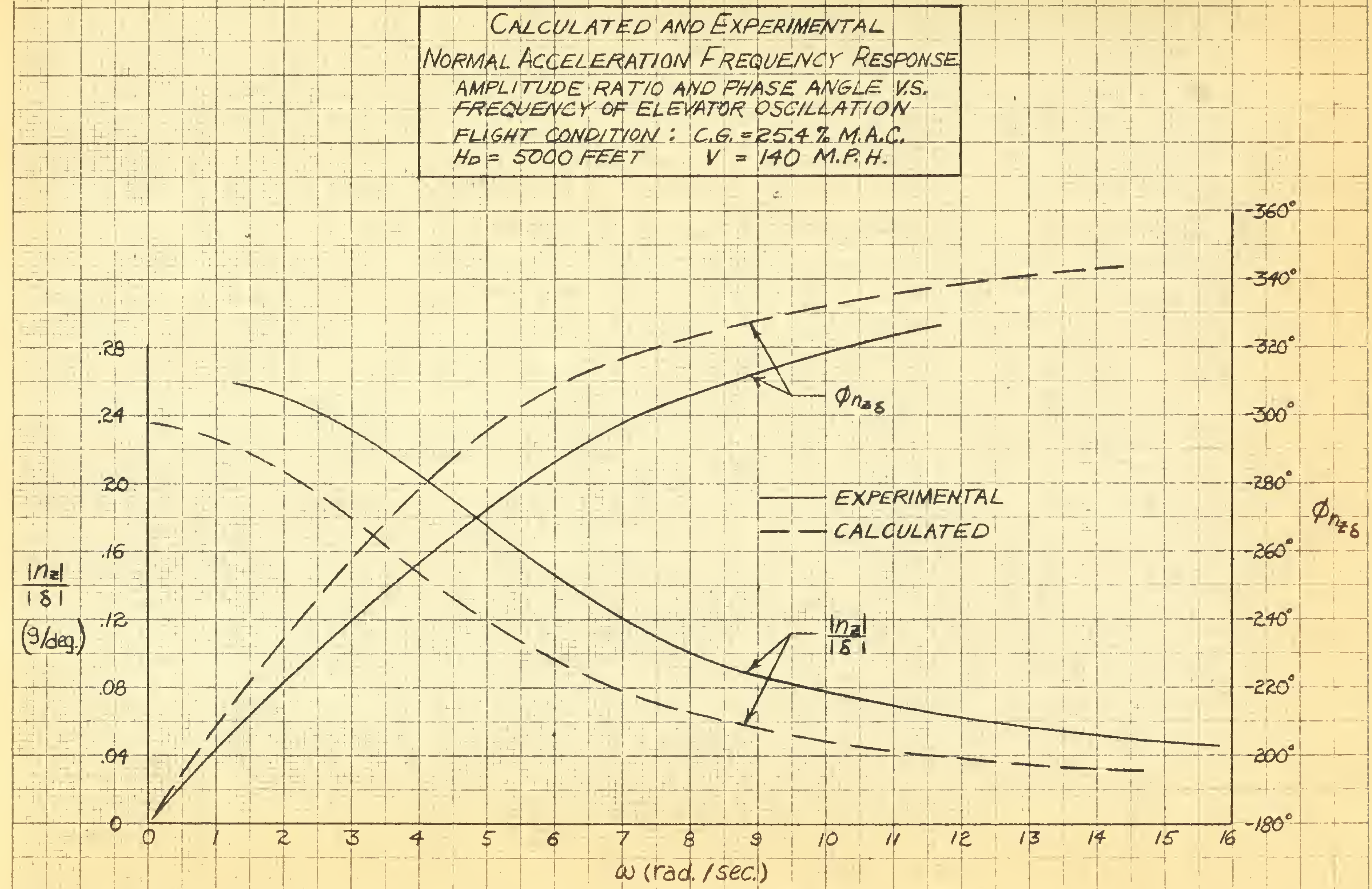

CALCULATED AND EXPERIMENTAL
NORMAL ACCELERATION FREQUENCY RESPONSE
AMPLITUDE RATIO AND PHASE ANGLE V.S.
FREQUENCY OF ELEVATOR OSCILLATION
FLIGHT CONDITION : C.G. = 25.4 % M.A.C.
H_D = 5000 FEET V = 140 M.P.H.

FIG. 24

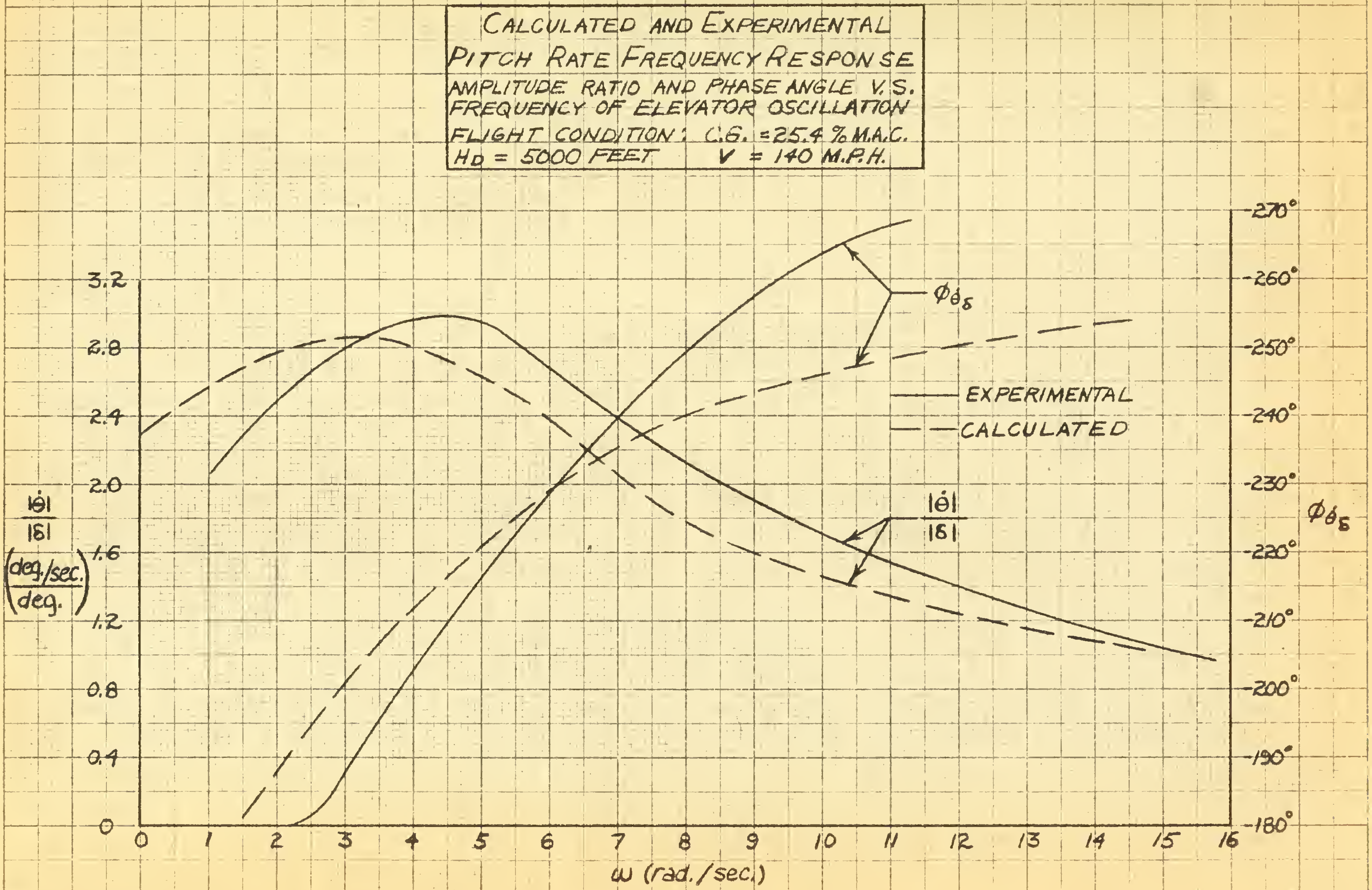
CALCULATED AND EXPERIMENTAL
PITCH RATE FREQUENCY RESPONSE
AMPLITUDE RATIO AND PHASE ANGLE V.S.
FREQUENCY OF ELEVATOR OSCILLATION
FLIGHT CONDITION: C.G. =25.4 % M.A.C.
H_D = 5000 FEET V = 140 M.P.H.

FIG. 25

COMPARISON OF NORMAL ACCELERATION
LINEARIZED SECOND ORDER TRANSFER FUNCTION
AND EXPERIMENTAL FREQUENCY RESPONSE
AMPLITUDE RATIO AND PHASE ANGLE V.S. FREQUENCY OF ELEVATOR OSCILLATION
FLIGHT CONDITION : C.G. = 25.4 % M.A.C.
H_D = 5000 FEET V = 140 M.P.H.

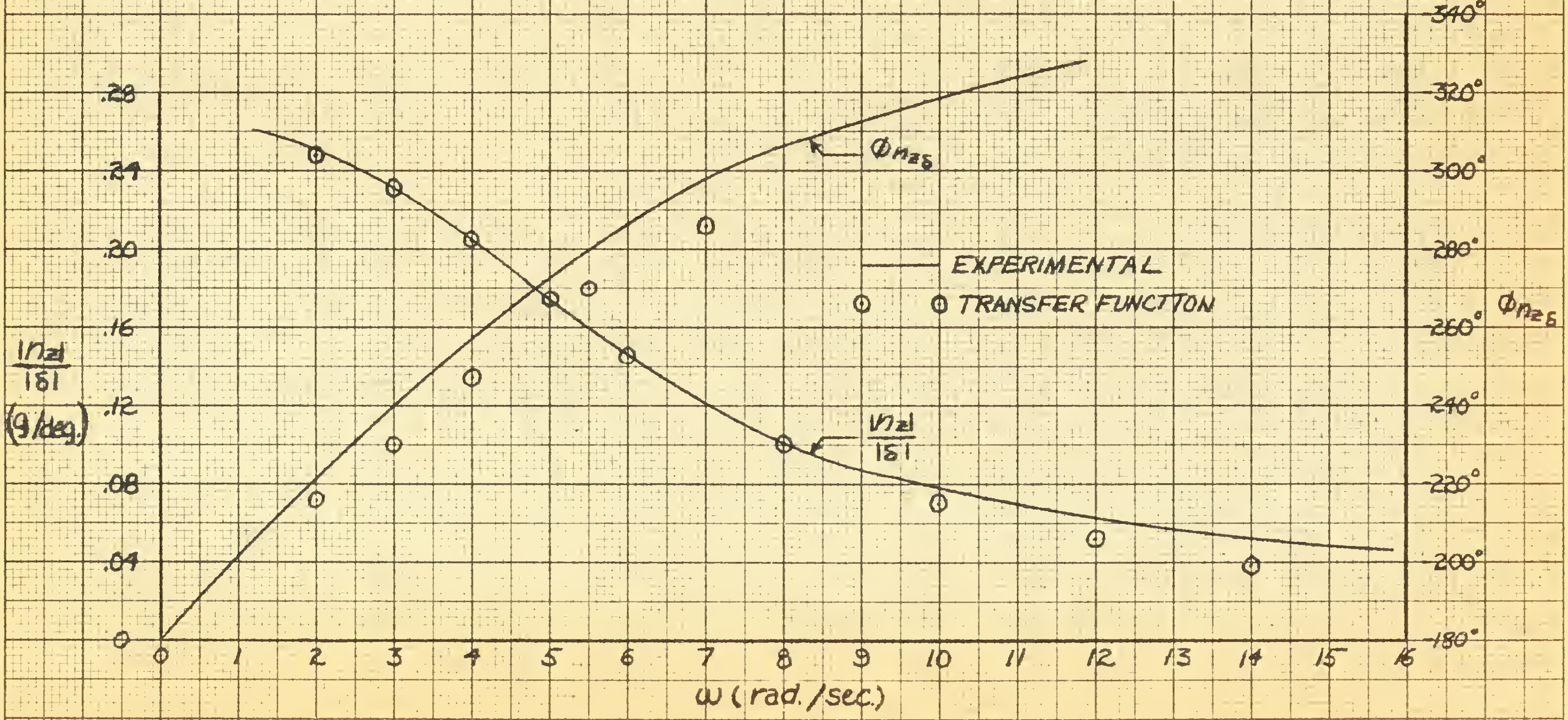

FIG. 26

COMPARISON OF PITCH RATE
LINEARIZED SECOND ORDER TRANSFER FUNCTION
AND EXPERIMENTAL FREQUENCY RESPONSE
AMPLITUDE RATIO AND PHASE ANGLE V.S.
FREQUENCY OF ELEVATOR OSCILLATION
FLIGHT CONDITION: C.G. = 25.4 % M.A.C.
H_D = 5000 FEET V = 140 M.P.H.

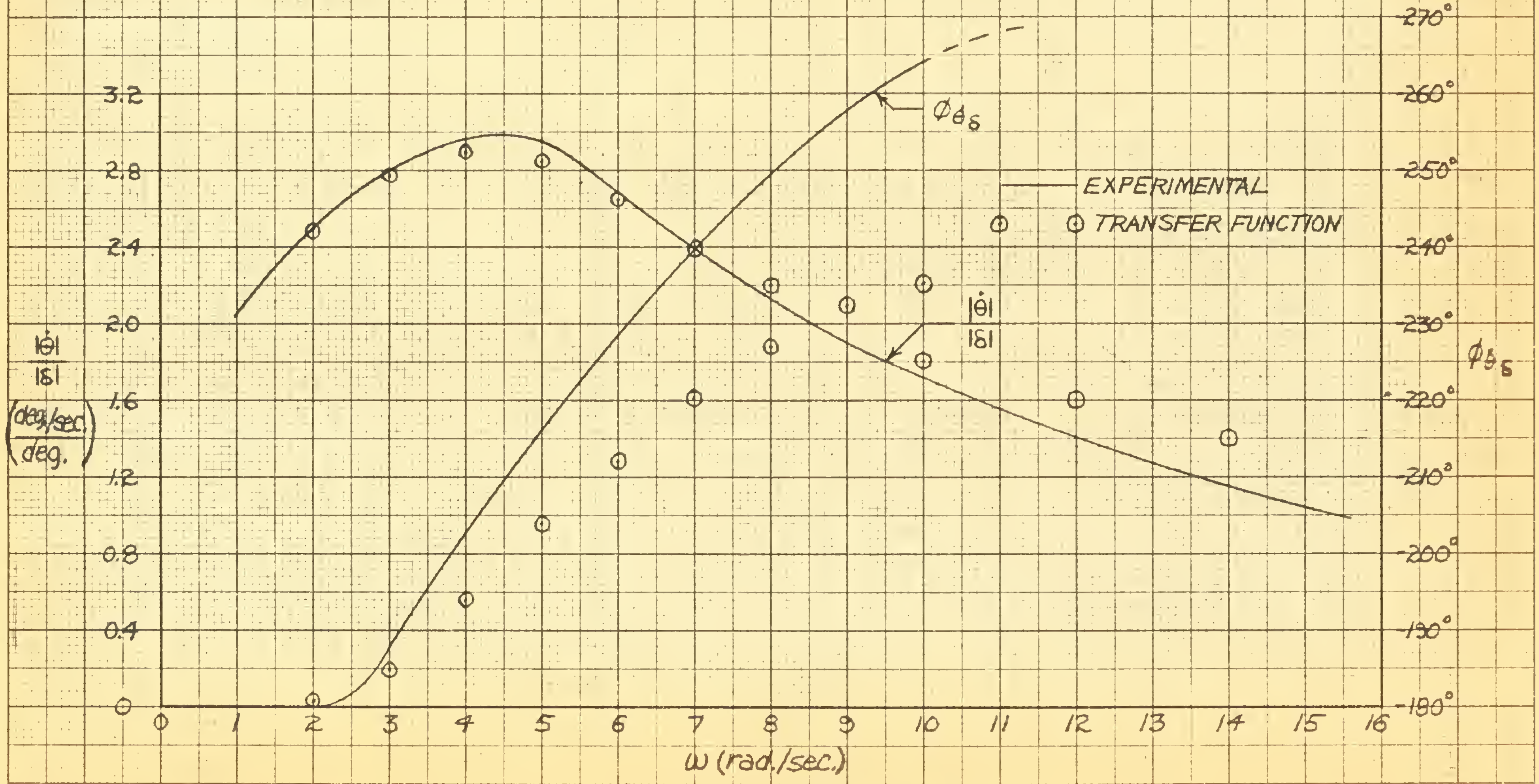

FIG. 27

Thesis
E278 23910
Eka
The longitudinal
frequency response of
a Navion airplane from
steady state dynamic
testing utilizing
simplified instrumenta-
tion.

Thesis
E278 23910
Eka
The longitudinal frequency
response of a Navion airplane
from steady state dynamic
testing utilizing simplified
instrumentation.

thesE278
The longitudinal frequency response of a
3 2768 001 90381 8
DUDLEY KNOX LIBRARY